

**STRUCTURAL AND DEPOSITIONAL EVOLUTION, KH FIELD,
WEST NATUNA BASIN,
OFFSHORE INDONESIA**

A Thesis

by

MARIA FRANSISCA MEIRITA

Submitted to the Office of Graduate Studies of
Texas A&M University
in partial fulfillment of the requirements for the degree of

MASTER OF SCIENCE

August 2003

Major Subject: Geophysics

**STRUCTURAL AND DEPOSITIONAL EVOLUTION, KH FIELD,
WEST NATUNA BASIN,
OFFSHORE INDONESIA**

A Thesis

by

MARIA FRANSISCA MEIRITA

Submitted to Texas A&M University
in partial fulfillment of the requirements
for the degree of

MASTER OF SCIENCE

Approved as to style and content by:

Joel S. Watkins
(Chair of Committee)

Steven L. Dorobek
(Member)

Walter B. Ayers
(Member)

Andrew Hajash, Jr.
(Head of Department)

August 2003

Major Subject: Geophysics

ABSTRACT

Structural and Depositional Evolution, KH Field,
West Natuna Basin, Offshore Indonesia. (August 2003)

Maria Fransisca Meirita, B.S., Trisakti University

Chair of Advisory Committee: Dr. Joel S. Watkins

This study describes the structural and depositional evolution in the KH field in West Natuna Basin, Indonesia. Data for the study were acquired by three-dimensional (3D) seismic reflection volume and a complete suite of well logs.

The regional basin underwent transtensional, sinistral shear during the rift phase that reactivated during the early to middle Miocene inversion as a traspressional, dextral shear. The study identified four periods of tectonic activity in the area which are extension, quiescence, compression and another period of quiescence.

A structural closure developed along a series of north-south trending, normal splay faults defines the area's trap play. Understanding how this structural play fits into the regional tectonic picture may suggest new approaches to hydrocarbon exploration in the area.

DEDICATION

To my Dad and Mom.

ACKNOWLEDGEMENTS

I would like to thank Dr. Joel S. Watkins, Chair of my Advisory Committee, for accepting me as one of his master's students and for his advice and support. I would also like to thank my committee members, Dr. Steven L. Dorobek and Dr. Walter B. Ayers, for serving on my committee, and for their valuable comments about my thesis.

I would like to acknowledge and express my appreciation to Gulf Resources Indonesia for providing me the seismic and well data which made this study possible and to Pertamina Consortium Study Abroad Program and Gulf Resources Indonesia (now under ConocoPhillips) for giving me the scholarship. Special thanks to Mr. Chuck Caughey for his support and guidance throughout my study.

Help along the way was provided by Rachmat Mudjiono, Mufti Irfan, Muadz Chalik, Anggarsih, Anggoro, Osman Suyud, Mike Lee, Rasheed, Tran, Gabriel, Joel Le Calves, Shirley, Amelia Reed, Ogtay, Choi, Rahadian, Fitrix, Munji and Yanyan.

Finally, I would like to express my sincere gratitude to my parents and my sisters, who have provided me with endless support throughout my life.

TABLE OF CONTENTS

	Page
ABSTRACT.....	iii
DEDICATION.....	iv
ACKNOWLEDGEMENTS.....	v
TABLE OF CONTENTS.....	vi
LIST OF FIGURES.....	viii
 CHAPTER	
I INTRODUCTION.....	1
II BACKGROUND.....	6
Previous work and geologic history.....	6
III METHODS.....	13
IV DEPOSITIONAL EVOLUTION.....	15
Rift-related linked depositional systems.....	15
Synrift megasequence.....	21
Postrift megasequence.....	26
Syninversion megasequence.....	26
Postinversion megasequence.....	27
Isochron maps.....	27
Basement-Lower Gabus interval.....	27
Lower Gabus-Upper Gabus interval.....	27
Upper Gabus-Barat interval.....	30
Barat-Base Muda interval.....	30
V STRUCTURAL EVOLUTION.....	33
Time-structure maps.....	33
Basement horizon.....	33
Lower Gabus horizon.....	35
Upper Gabus horizon.....	35

CHAPTER	Page
Barat horizon.....	35
Base Muda Unconformity horizon.....	39
Basement fault.....	39
Extension and inversion.....	39
VI DISCUSSION.....	49
Model of basin development placed in regional context.....	49
Prospective traps.....	50
VII CONCLUSIONS.....	51
REFERENCES CITED.....	53
VITA.....	56

LIST OF FIGURES

FIGURE	Page
1 KH field location within Natuna Sea Tertiary basin map.....	2
2 KH field seismic lines and well locations shown in the study area	5
3 Schematic map of Cenozoic extrusion tectonics is modified from Tapponier et al., (1982)	7
4 Schematic structural development, West Natuna Basin from Roberts (1988).....	9
5 Chronostratigraphic KH field modified from Gulf Resources (Kakap) Ltd., (2000).....	11
6 Four megasequences shown in the study area	16
7 Rift initiation system tract: (a) generalized block diagram; (b) schematic cross-section from Prosser (1993).....	18
8 Rift climax system tract: (a) generalized block diagram; (b) schematic cross-section from Prosser (1993).....	19
9 Immediate post-rift systems tract; (a) generalized block diagram; (b) schematic cross-section from Prosser (1993).....	20
10 Late post-rift system tract: (a) generalized block diagram; (b) schematic cross-section from Prosser (1993).....	22
11 Seismic section profile (a) and its line interpretation (b) showing rift initiation (S2), rift climax (S3), immediate post rift (S4) and late post rift (S5).....	23

FIGURE	Page
12 Isochron map of Basement – Lower Gabus interval.....	28
13 Isochron map of Lower Gabus – Upper Gabus interval.....	29
14 Isochron map Upper Gabus – Barat interval	31
15 Isochron map Lower Gabus – Base Muda Unconformity interval	32
16 Time-structure map of Basement.....	34
17 Time-structure map of Lower Gabus.....	36
18 Time-structure map of Upper Gabus.....	37
19 Time-structure map of Barat.....	38
20 Time-structure map of Base Muda Unconformity.....	40
21 The schematic illustration of distributed continental deformation in the formation of extensional basins in the study area	42
22 Block model for extension and inversion in the study area based on original concept of McKenzie and Jackson (1986).....	42
23 Line 1 showing fault-propagation fold or sunda fold.....	43
24 Structural development of Sunda fold features in study area.....	44
25 Line 2 showing series of normal fault that develop during inversion and basement fault.....	45
26 Line 3 showing series of normal fault and basement fault.....	46
27 Line 4 showing synthetic and antithetic faults and basement fault.....	47
28 Line 5 showing series of normal faults.....	48

CHAPTER I

INTRODUCTION

The KH field is located in the northwest corner of the South Kakap Production Sharing Contract area in West Natuna Basin (Figure 1), Indonesia, approximately 200 km northwest of Natuna Island and over 1000 km north of Jakarta, Indonesia. The total area of Kakap PSC is 2006 km² and water depth ranges from approximately 290 ft in the southern block to 190 ft in parts of the northern block.

The West Natuna Basin located in the South China Sea is bounded on the south and west by the Indo-Australian plate. The West Natuna Basin is dominated by a series of nonmarine extensional grabens and half-grabens that formed in the late Eocene to Oligocene and underwent inversion in the early to middle Miocene. The development of those extensional rift basins may have been influenced by far-field tectonics of the India-Australian collision. Tapponier et al. (1982) postulated that the India-Asian collision during the middle-late Eocene had caused Indochina to extrude southeastward along major strike-slip fault zones. The extrusion formed the extensional basins in West Natuna Basin. This extensional event created northeast-southwest trending grabens and half grabens.

This thesis follows the style of the American Association of Petroleum Geologists Bulletin.

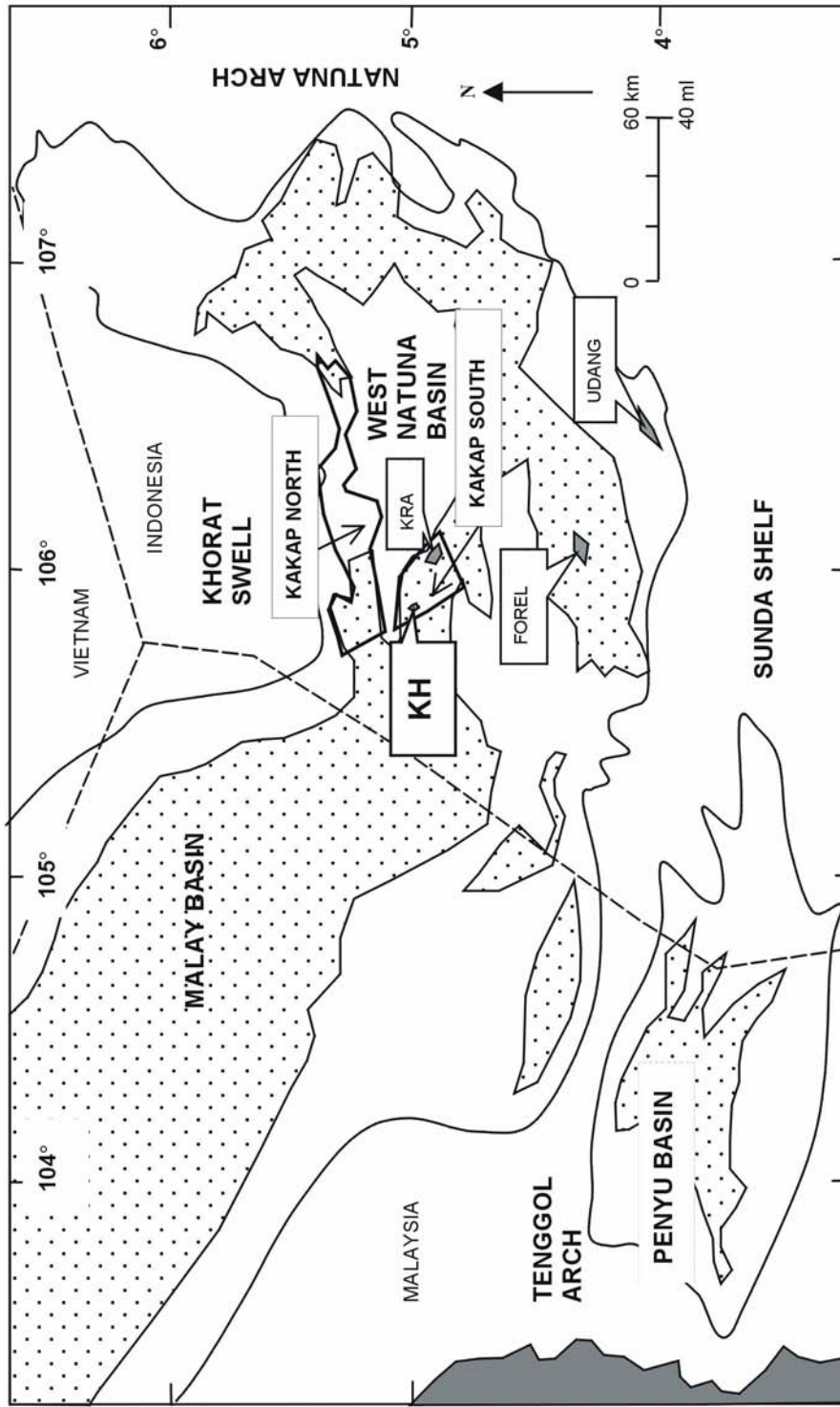


Figure 1. KH field location within Natuna Sea Tertiary basin map.

Inversion occurred on a large scale in the Kakap area in the early and middle Miocene inverting part of the basin. This produced many examples of what are known as Sunda folds in the Kakap area and elsewhere in the Indonesian region.

Tectonic history and depositional response in this area closely related. Throughout the rifting phase in the Eocene to early Oligocene the rift basin filled with lacustrine and fluvial sediments characterized by abrupt thickness variations. Normal faulting and basin subsidence exemplify this early stage of tectonic activity. During the early Miocene compression, widespread compressional tectonic activity began in the Kakap area. This era was also marked by the return of marine conditions. Marine conditions prevailed until the late-middle Miocene, when major compressional events terminated deposition and resulted in the regional Base Muda unconformity.

Hydrocarbons were discovered at KH field in 1980 in the upper sand of the Upper Oligocene Gabus Formation at the KH-1X well. The KH-2X well encountered three oil-bearing sands. Other wells also encountered hydrocarbons. Production tests in the KH-1X well reached rates of 7527 BOPD. The upper pay horizon is overlain by a gas cap.

The objective of this study is to describe the structural and depositional evolution in the KH field. Knowing the depositional evolution and structural framework may yield new ideas and approaches to exploration.

This study applied three-dimensional (3-D) seismic data and well logs to interpret deposition and structural relationships within the formation in KH field. The seismic data were acquired by Marathon Petroleum Indonesia during March and April 1992 and were provided for this study by Gulf Indonesia Resources, Ltd. The seismic consist of 600 inline and 500 crossline with CDP is 12.5 m (Figure 2).

The well-log database for this study comprises five delineation wells within the 3-D survey area. Maximum depth is 9280 ft. Well log traces including gamma ray, resistivity, density, and sonic logs, were integrated with the seismic data. Four lithologic “tops” and one unconformity marker were identified on the logs.

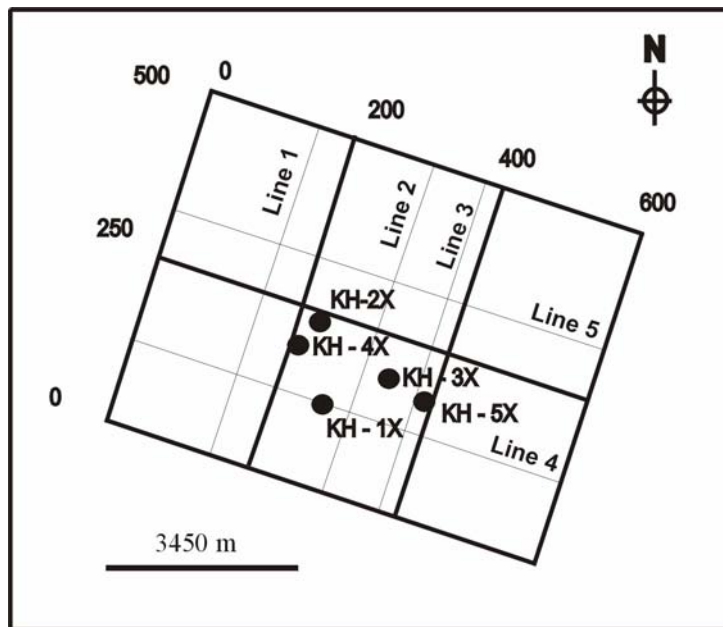


Figure 2. KH field seismic lines and well locations shown in the study area.

CHAPTER II

BACKGROUND

Previous work and geologic history

Previous worker in this area report, that tectonic inversion is responsible for the modern structure. This inversion ranged from extension to compression, and it reactivated previous structures. Some authors (Roberts, 1988 and Ginger et al., 1993) suggested that wrench deformation of the basin controls the sediment deposition in this area.

West Natuna Basin is bounded by the Khorat-Con Son Swell on the north, by the Natuna Arch on the east, by the Tengol Arch on the west and by the Sunda Shelf on the south (Figure 1). Several regional tectonic models have been proposed for development of the basins in this Sunda shelf area. For example, Tapponier et al. (1982), proposed extrusion tectonics and southeastward translation resulting from the collision between India and Eurasia that caused Indochina and adjacent offshore areas to extrude and rotate clockwise (Figure 3). Daly et al. (1990) assumed that the indentation of the Indian Plate into the Asian Plate transmitted stress by rotation of the Sumatra Subduction zone. This rotation generated a right-lateral strike-slip couple that resulted in extension, which in turn created half grabens. Tjia and Liew (1996) suggested transtensional stress and northeast-southwest sinistral shear caused by wrenching that also created Paleogene rifting.

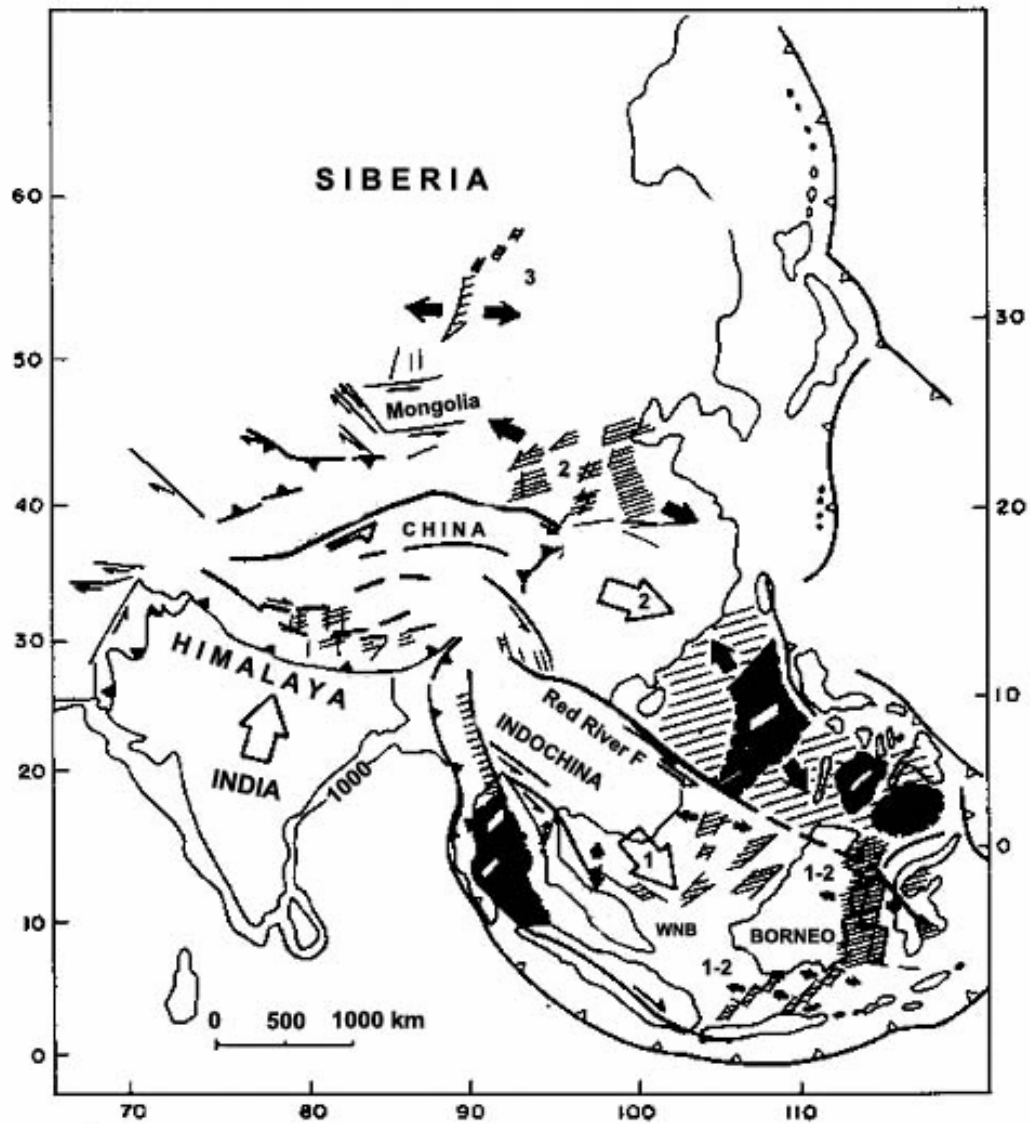
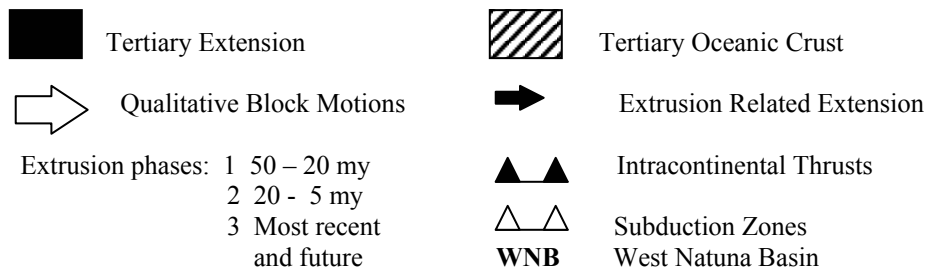


Figure 3. Schematic map of Cenozoic extrusion tectonics is modified from Tapponier et al. (1982).



Roberts (1988) categorized West Natuna Basin as a wrench-related basin that developed along a major zone of transcurrent or transform fault movement extending from northern Burma to the Junction of the Red River Fault and the North Borneo Trench offshore Sarawak. Basin geometry was created by continuous opening of pull-apart basins in response to extrusion tectonics. The evolving geometry and architecture of a typical pull-apart basin at West Natuna Basin are shown in Figure 4.

Sunda folds are common central Sumatra and elsewhere on the Sunda shelf, including in the study area. Eubank and Makki (1981) define a Sunda fold as an inverted fold caused by wrench deformation of an earlier normal-faulted section. Sunda Folds tend naturally to be fault-bounded, shallow anticlines that are synclinal or half graben at depth. The characteristics of these structures are as follows:

1. Sediment thickness increases over the structure.
2. Fold amplitude decreases with depth, often becoming synclinal at basement level.
3. Throw of the major bounding fault reverse with depth. The upper part of the fault shows reverse movement and the lower part shows normal throw.

In their study of petroleum geology in KH field, Pollock et al. (1984) define a structure that outlines the area as an asymmetric compressional fold that conveys to a northwest-southwest-trending, right-lateral, strike-slip fault. This strike-slip movement is an overprint onto the earlier rifting phase. The fold was bisected by a north-south-trending, normal, listric fault dipping westward. Paleontological data show that the

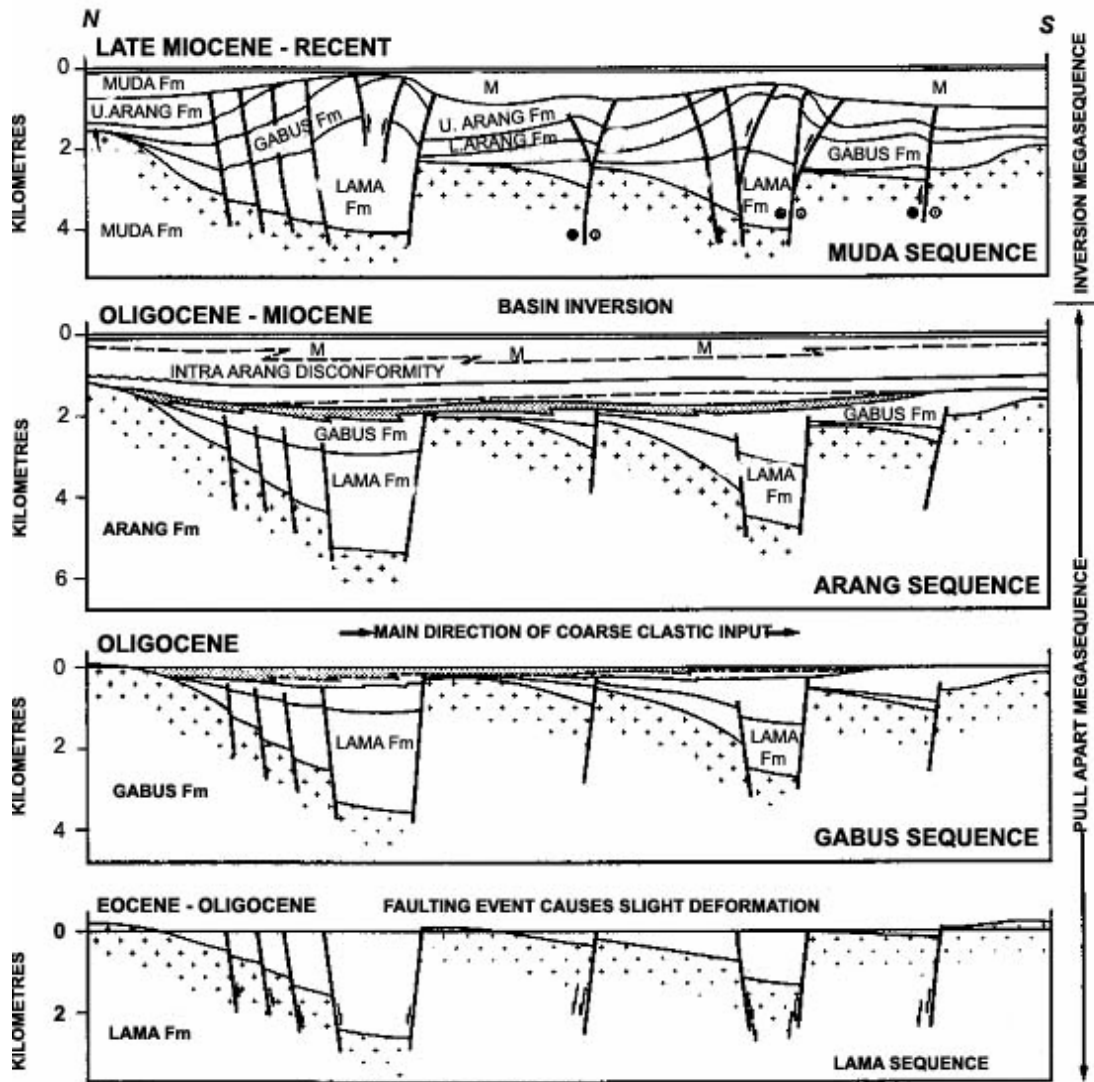


Figure 4. Schematic structural development, West Natuna Basin from Roberts (1988).

compressional event responsible for the present structural configuration in the area is mid-Middle Miocene.

Formation of the West Natuna Basin began during the late Eocene to the early Oligocene which extension generated a complex of east-west to northeast-southwest half grabens. This period is described as a synrift megasequence on the basis of the tectonic processes active during the deposition of the various sedimentary units (Figure 5). The rift basin filled with lacustrine to fluvio-deltaic and alluvial sediments (Lama and Benua Formations). This is construed to have been a time for the development of lacustrine source rocks in the rift depocentres (Gulf Resources (Kakap) Ltd., 2000).

The postrift megasequence (early to late Oligocene) consisted of a period of tectonic quiescence. Erosion of the stable shelf area supplied relatively thick, coarse clastics of the Gabus formation. High-energy braided fluvial systems developed at a number of levels, while silts and shales were deposited in lower energy distal fluvial/lacustrine environment (Gulf Resources (Kakap) Ltd., 2000).

Change in orientation of regional stress fields (early to middle Miocene) marked the syninversion megasequence. This change in stress resulted in compressional and

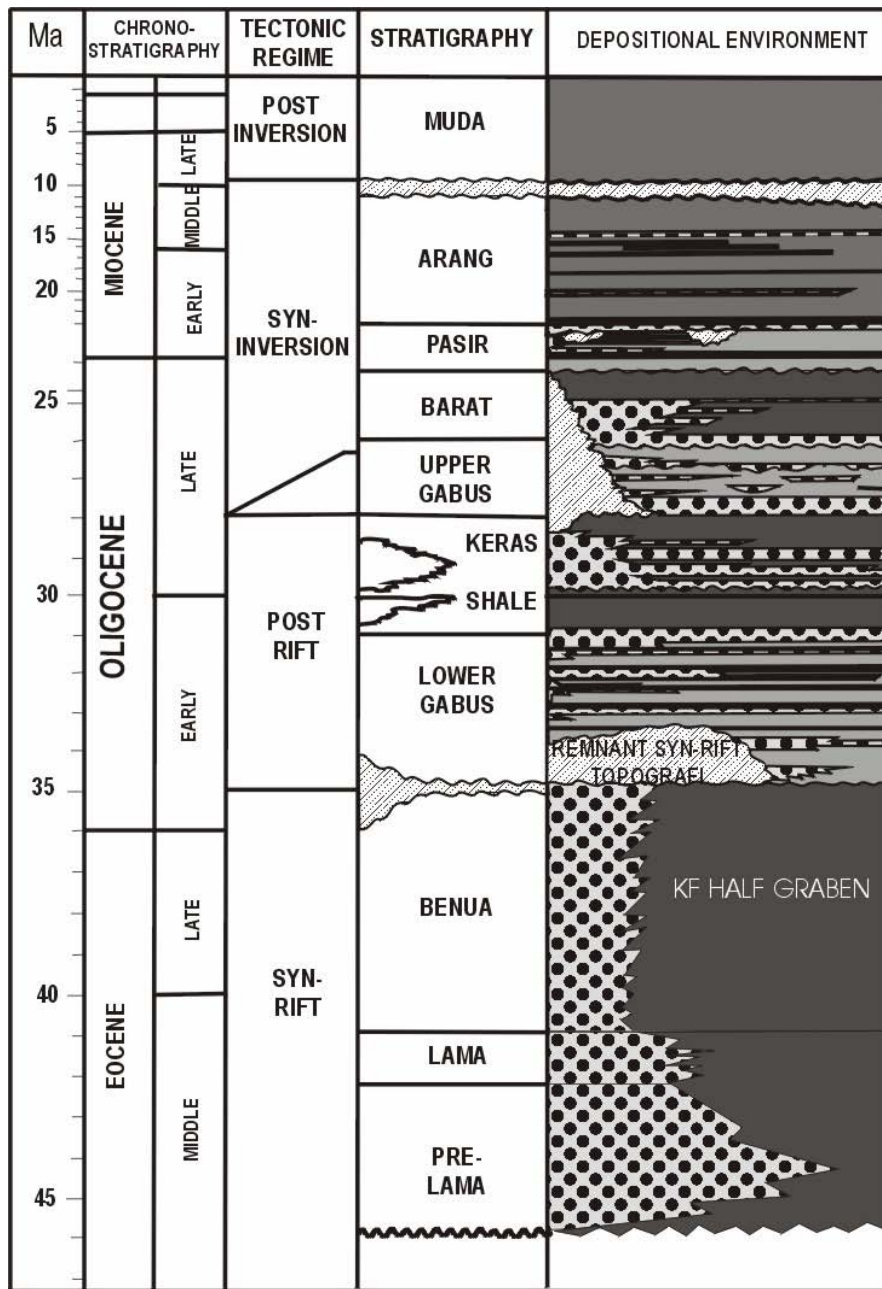


Figure 5. Chronostratigraphic KH Field modified from Gulf Resources (Kakap) Ltd., (2000). Depositional environment:

- Shallow - deep marine
- Lacustrine margin
- Lacustrine (shale - dominated)
- Fluvio-deltaic

transpressional stress in this basin. Tjia and Liew (1996) proposed that this change of stress was caused by cessation of the spreading of the South China Sea basin, which enabled the westward convergence of the Pacific plate in the middle Miocene and the convergence of the Indian-Australian plate from the south at the end of the Miocene.

Compressional and transpressional stress inverted major basin-bounding faults and formed anticlines over hanging-wall blocks of the reverse faults (Wirojudo and Wongsosantiko, 1985). East-northeast trends of anticlinal folds suggest a northwest-southeast maximum horizontal stress (Tjia and Liew, 1996). A number of transgression-regression cycles defined the deposition during this period.

This sequence of cycles resulted in a depositional environment that fluctuated from lacustrine (Barat) to marginal marine (Pasir) and coal-swamp dominated coastal plain (Arang). Some of this cycle may have occurred because of inversion events whereas other cycles were caused by changes in regional relative sea level (Ginger et al., 1993). Inversion continued until the late Miocene, when the Base Muda Unconformity developed.

Postinversion Muda Formation is marked by shale domination in shallow marine to paralic sequences. Faulting was not present in this period.

CHAPTER III

METHODS

This project used state-of-the art computer workstation techniques to facilitate data integration and interpretation. I used Schlumberger Geoframe Charisma software to interpret and manipulate seismic data and well-log information.

The data used in this study are 3D seismic in KH field, which consist of 600 inlines and 500 crosslines. The seismic grid is oriented north-northeast and west-northwest. Record length is 3.5 seconds TWT. The seismic data are zero-phase. The polarity convention adopted for all of the seismic displays is that a positive reflection coefficient (increase in acoustic impedance) represents a trough. Alternatively, a negative reflection coefficient is a peak. The variable area display used for this study is red-white-black.

I correlated a grid of data from the 3D survey consisting of approximately every tenth crossline and inline. I also generated time slices to aid in interpretations. I did structural interpretation by picking fault patterns and horizon continuations.

Since fault displacement can be vertical, lateral or some of each, to interpret the fault we should know the best angle to look at it. Subvertical faulting is seen best on vertical seismic sections, while lateral (strike slip) faults are better seen in horizontal sections.

In this study, I mapped major faults in vertical sections and horizontal sections. In vertical sections, faults are identified by aligned bed termination, abrupt dip change, and aligned dim amplitude (fault shadow), while in horizontal sections faults are identified by lateral displacement of amplitude bands.

Seismic horizons were picked within the data set on the basis of the lithologic tops and unconformity markers identified on the logs. The auto track from Charisma was used while picking the horizons. This enabled selection of the true maximum or minimum amplitude associated with each particular horizon. I used jump correlation when picking events across faults. When there is inconsistency with this seismic jump correlation across faults, then well-tie correlation became a key to correct it. The final product is a time-structure, colored-grid map. This map depicts structural highs, lows, and fault trends, outlines potential structural trap; and helps define structural controls on deposition. I also created the Isochron maps for every horizon interval to show the variation of sediment thickness.

Four major tectonostratigraphic units were also identified within the study area to highlight the different tectonic processes active during the deposition of the various sedimentary units.

CHAPTER IV

DEPOSITIONAL EVOLUTION

Rift-related linked depositional systems

In the study area where fault movement is in response to extensional tectonic forces (Pollock et al., 1984; Ginger et al., 1993), the strength of the tectonic signature becomes the dominant factor in the control on sedimentation. In terminal asymmetric basins, bounded by faults that move in response to extensional tectonic forces, facies relationships include features that may be related to influences that are solely local-tectonic in origin, and that could not be due to a more regional change in relative base level (Prosser, 1993). The duration of each rift-related linked depositional system, and the sequences they form part of, will depend on the rate of faulting and basin formation, which may be highly variable. In this case where the linked depositional systems would be tectonic in origin, tectonic systems tracts might be define (Prosser, 1993).

Four tectonostratigraphic megasequences identified in the study area showing the different tectonic processes active during the deposition of the various sedimentary units (Figure 6). The four megasequences are synrift, postrift, syninversion and postinversion. A unique association of sequence geometry, facies associations and reservoir architecture characterize each phase. A prerift sequence is deposited prior to any extensional movement. A synrift sequence is deposited during extensional faulting or rift-basin infill. A postrift sequence is deposited after the cessation of extensional

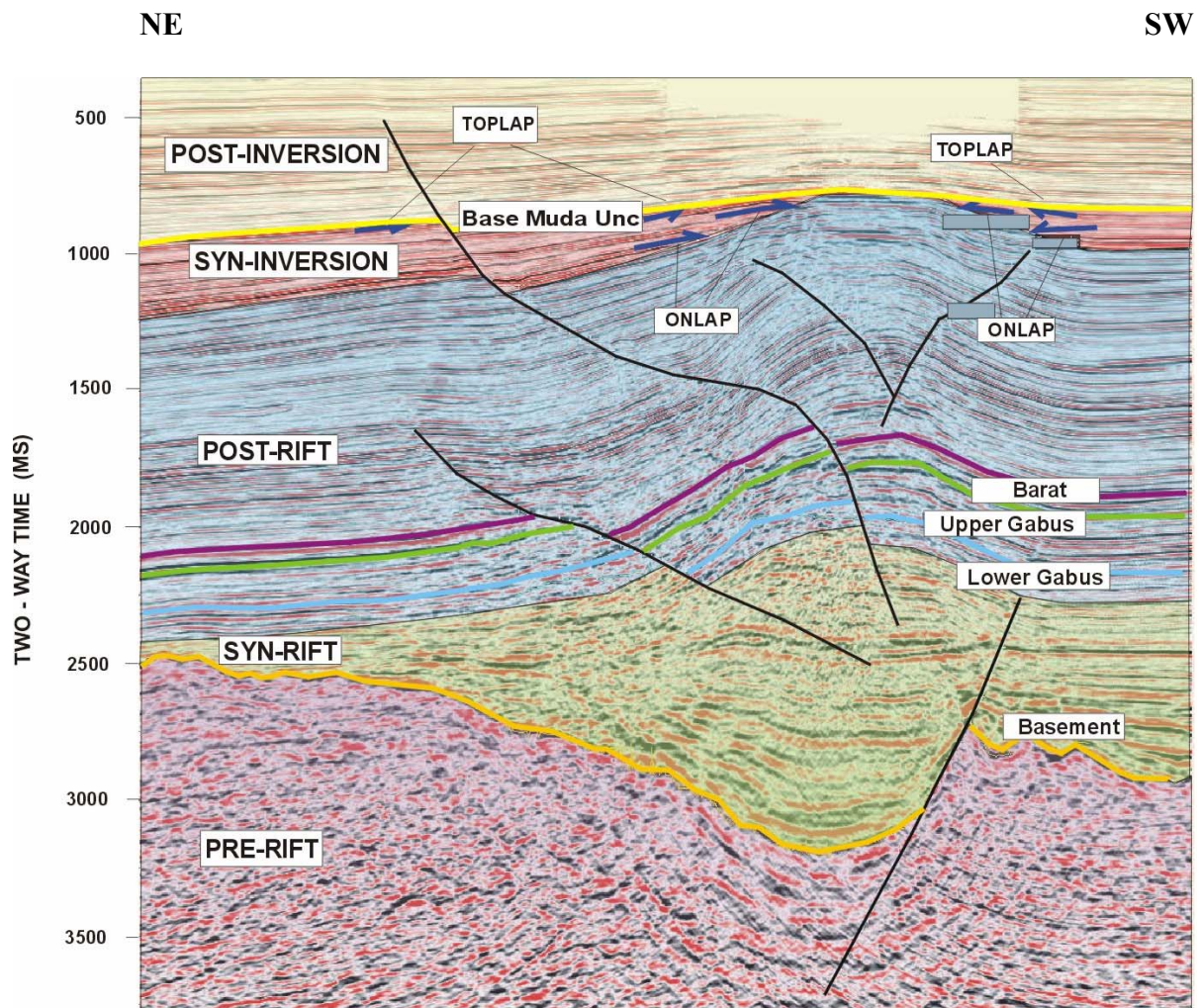
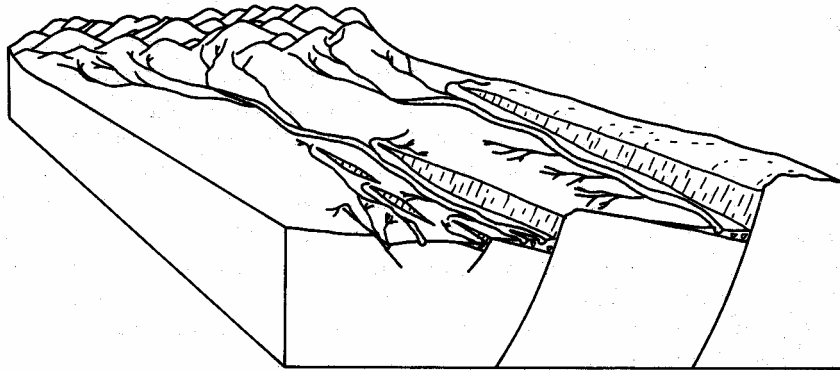


Figure 6. Four megasequences shown in the study area.

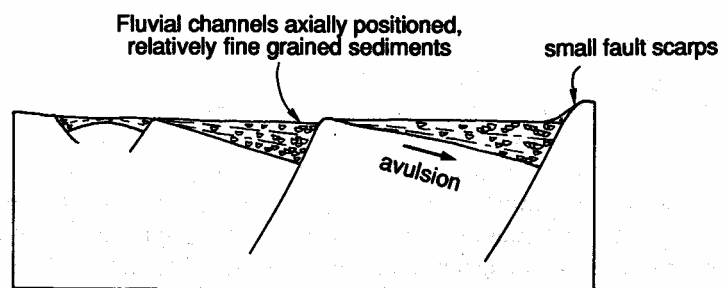
faulting. The postrift sequence may be deposited after a period of non-deposition and/or erosion marked by a break-up unconformity, which may remove part of the synrift sequence (Williams et al., 1989). A syninversion sequence is deposited during inversion and a post-inversion sequence is deposited after the inversion.

Prosser (1993) explains the stages of rift evolution that occur in active-fault bounded basins. Rift initiation (S2) is the first increment of movement on a fault cause a depression in the crust's surface to which gravity-driven sedimentary systems will respond (Figure 7). For the purposes of tectonic systems tract description the basin is presumed at this stage to be sub aerial, with enough water supply to maintain perennial fluvial systems, and the surrounding source areas to be composed of consolidated, competent rock. A rift climax (S3) is the time of maximum rate of displacement on a fault (Figure 8). Three stages (early, mid and late), each a separate systems tract, was described for rift climax. Immediate post-rift or immediate late syn-rift (S4) is the end of active tectonism and displacement on the basin-bounding fault (Figure 9). Late postrift or late synrift (S5) is the final response to the creation and infilling of a rift basin. It will be the gradual and slow peneplanation of the topography created through faulting. The late synrift systems tract may be masked by subsequent tectonic events, but in some

Key points: subsidence = sedimentation
no established drainage basins in newly created topographic locations
dominantly axial input from antecedent mature drainage basins
small isolated sub-basins, small area for deposition



(a)



(b)

Figure 7. Rift initiation system tract: (a) generalized block diagram;
 (b) schematic cross-section from Prosser (1993).

Key points: subsidence > sedimentation
 minor sediment accumulation due to increase in rate of subsidence (related to fault growth), increase in area for deposition, hydrological control (small drainage basins, canyon cutting, nick point migration mechanism)
 Unlikely to record minor eustatic changes

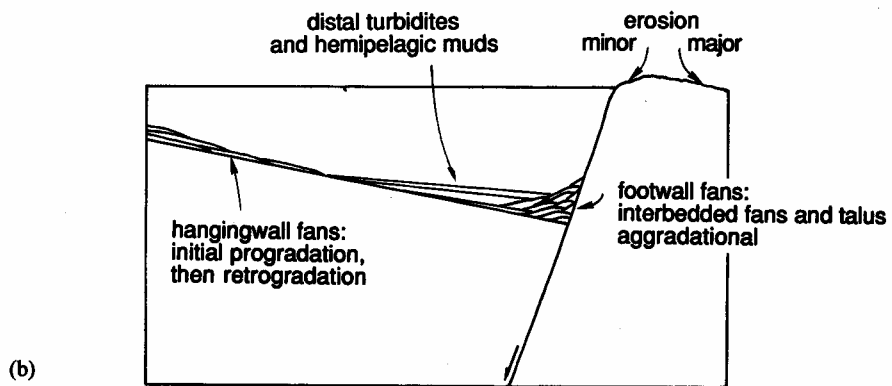
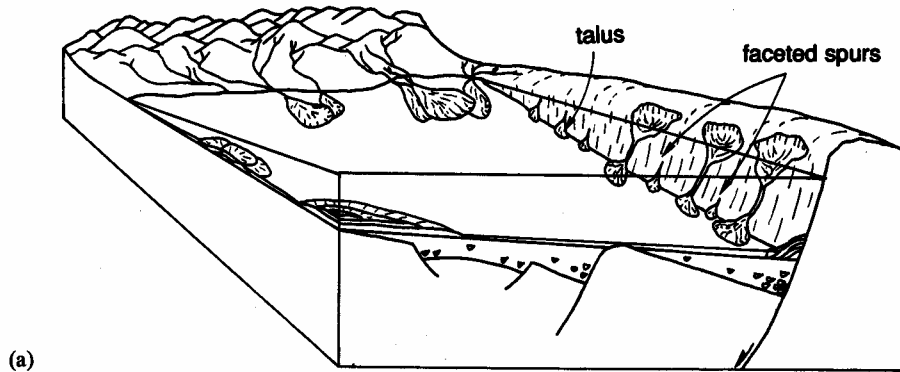


Figure 8. Rift climax system tract: (a) generalized block diagram; (b) schematic cross-section from Prosser (1993).

Key points: subsidence < sedimentation
 increase in general grain size due to expansion of footwall
 drainage basins, increase in progradation, filled to spill
 point. More likely to record minor eustatic changes.

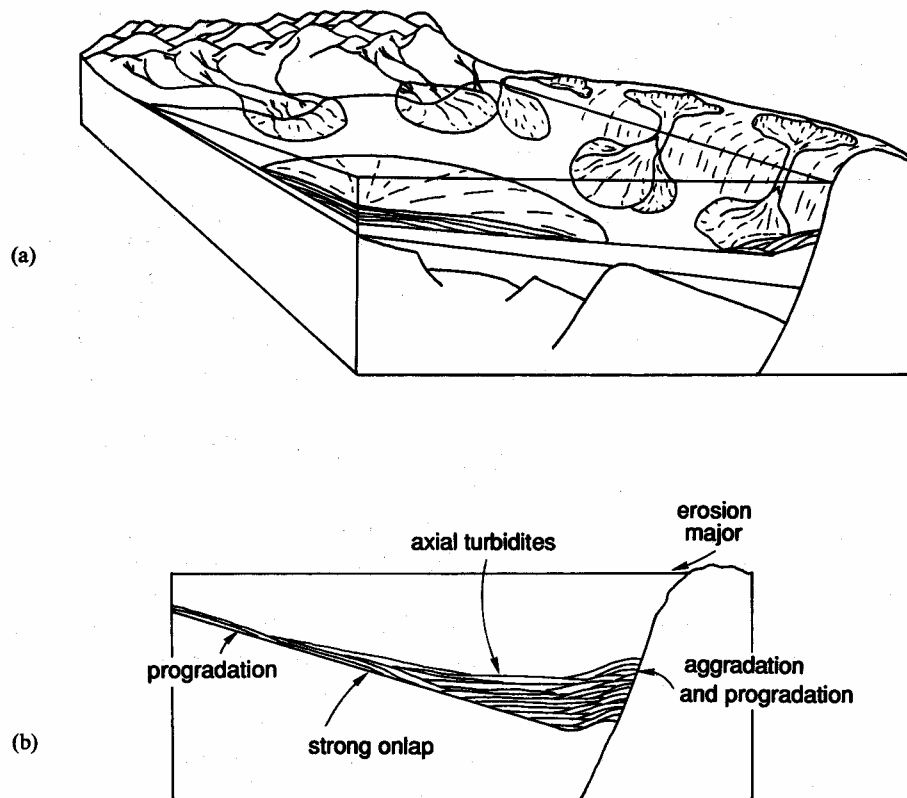


Figure 9. Immediate post-rift systems tract; (a) generalized block diagram; (b) schematic cross-section from Prosser (1993).

cases characteristic linked depositional systems may develop (Figure 10).

Three stages of rift evolution (rift initiation, rift climax and late synrift) were used to seismically subdivide the synrift megasequence in the study area. Each stage performs a distinct linkage of depositional systems and a seismic expression that enables its recognition on reflection profiles.

Synrift megasequence

Rift initiation (S2)

The reflection geometries in the study area illustrate some of the main characteristics of rift-initiation systems tracts on seismic section. Figure 11 shows an overall wedge-shaped geometry. The wedge shape has thin end that lies high on the hangingwall dip-slope. The internal reflector characteristics are generally discontinuous. The wedge shape reflects that the sedimentation kept pace with subsidence. A small fault scarps also shows on seismic section. This feature indicates the erosion of the footwall.

Rift climax (S3)

Generally, this stage shows the aggradation, progradation and retrogradation configuration together with the expansion of divergent forms. Three stages (early, mid and late-rift climax), each a separate systems tract can be described. Characteristic reflector geometries were shows mark of the onset and termination of the three different rift climax systems tracts that described below.

Key points: subsidence \neq sedimentation
 fine grained sedimentation due to degradation of fault scarp
 and continued thermal subsidence drowning major subaerial
 drainage basins.
 Eustatic signature more likely to be recorded.

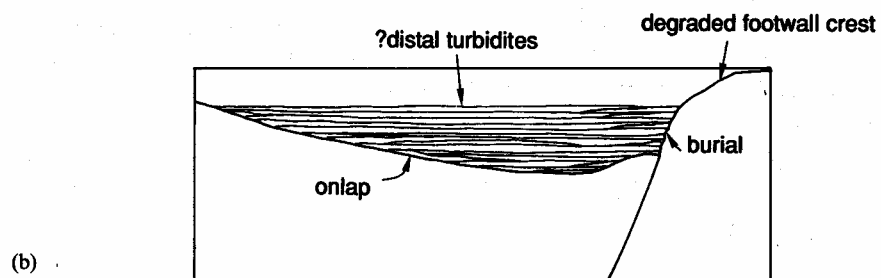
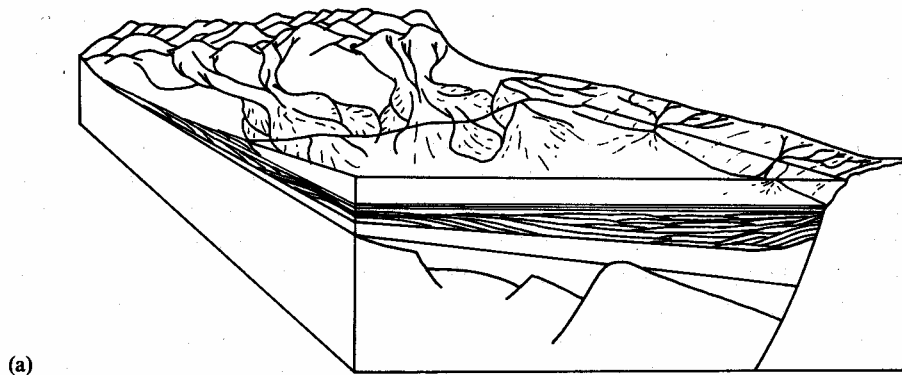


Figure 10. Late post-rift system tract: (a) generalized block diagram;
 (b) schematic cross-section from Prosser (1993).

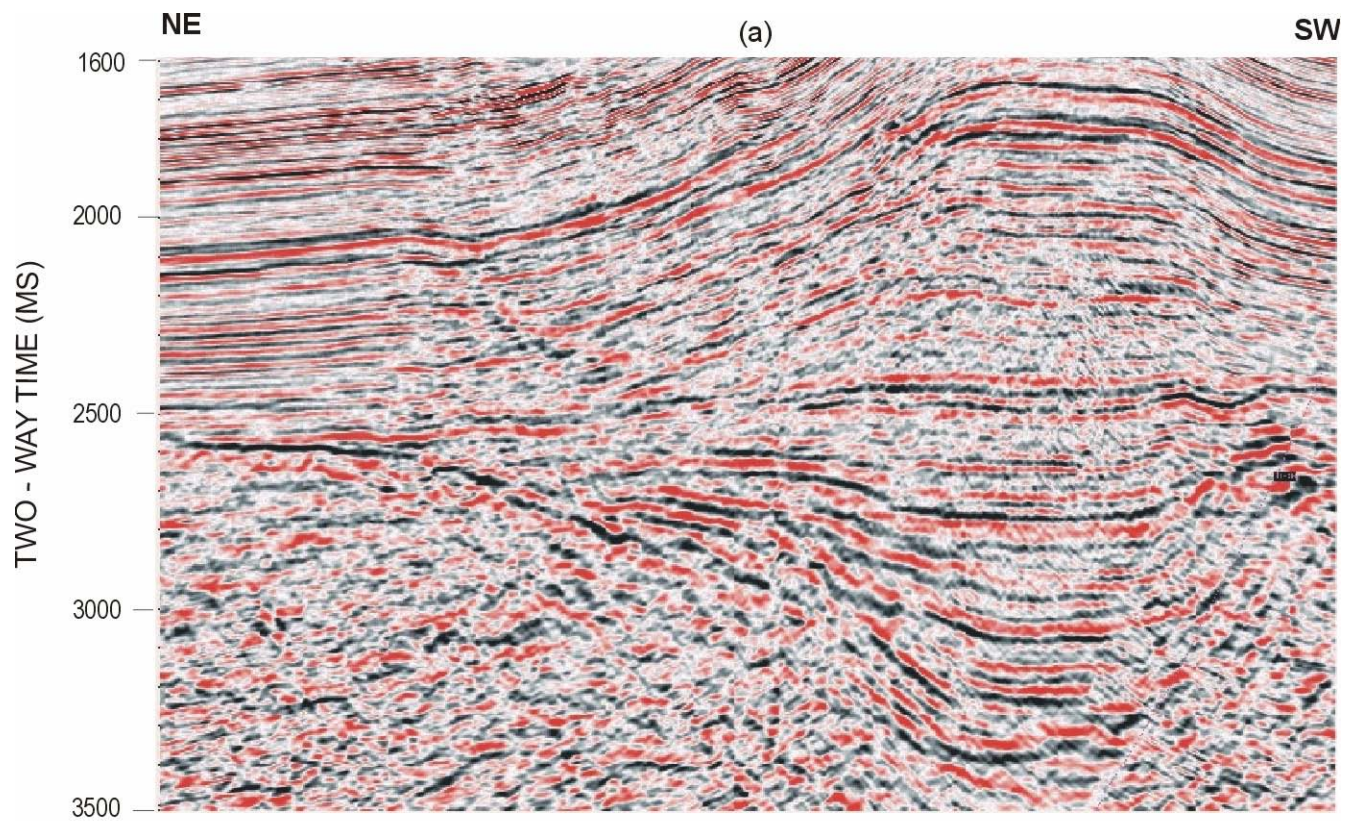


Figure 11. Seismic section profile (a) and its line interpretation (b) showing rift initiation (S2), rift climax (S3), immediate post rift (S4) and late post rift (S5).

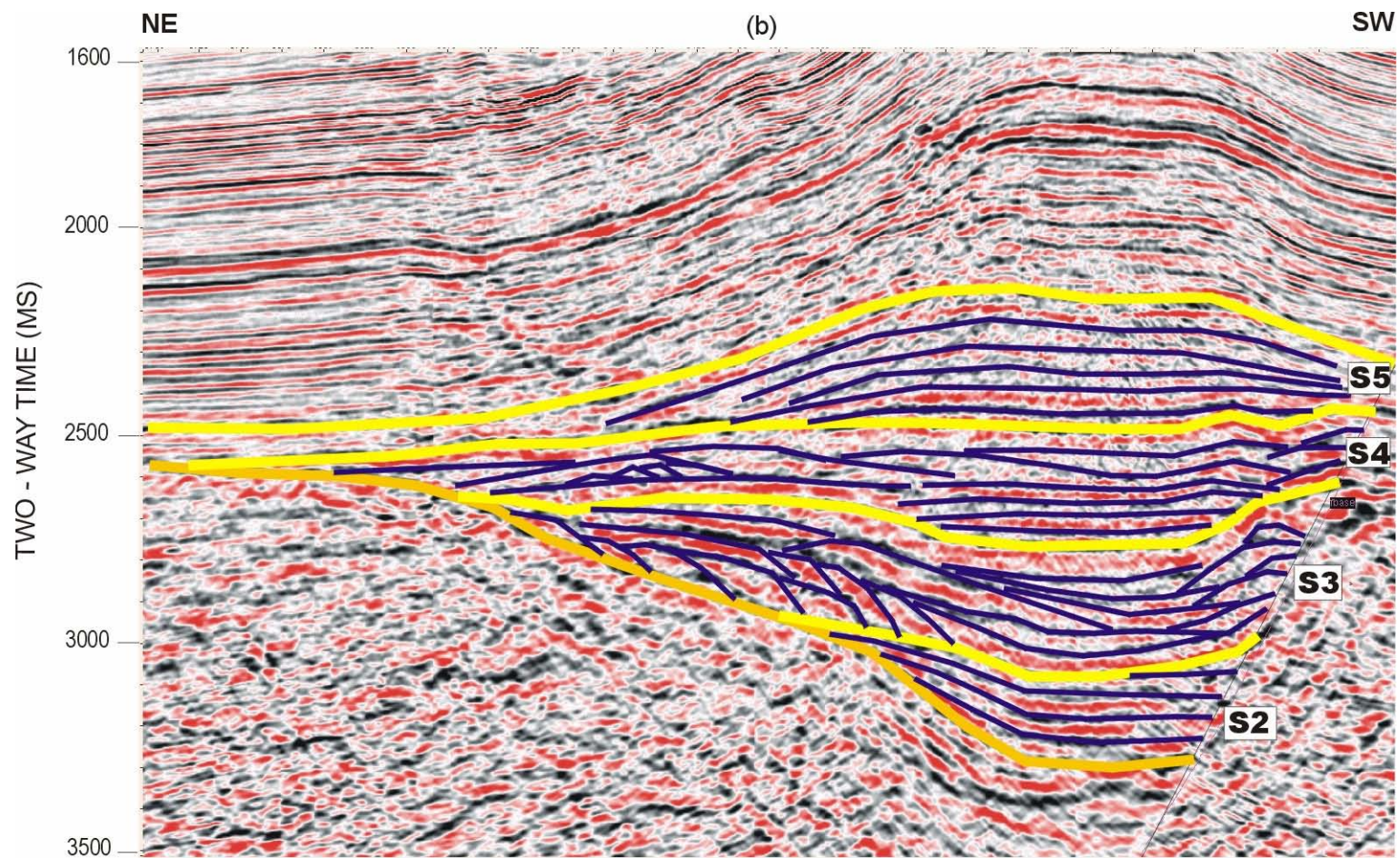


Figure 11. (continued).

Early rift climax system tract

The downlap surface shows the beginning of rift climax that discriminated this stage from the rift initiation (Figure 11). The progradation and offlap on hangingwall and aggrading reflectors close to the footwall characterize this stage. These forms show that transgression was occurred. The offlap on hangingwall demonstrates the successive tilting increments in basinward direction (Hunt & Mabey 1966; Hooke 1972; Leeder & Gawthorpe 1987) and forced shoreline regressions (Udall & Nolan 1964).

Mid-rift climax system tract

This stage in the study area is characterized by the retrogradational geometries of the reflectors on the hangingwall dip-slope, and the continuation of aggradation of the footwall sequences. The retrogradation reflects the low angle of dip on hangingwall and rapid drowning. A slightly divergence form shows in this stage. The divergence has continuous reflectors that diverge towards the fault plane. The footwall systems by aggradation of the footwall sequences had become important in the later stages of development (Figure 11).

Late rift climax system tract

A draping reflector shows on seismic section in the study area (Figure 11). This draping reflector shows the decrease of sediment accumulation rates. The depositional system predominates in a totally submerged environment.

Immediate post-rift (S4)

The infilling reflector package has the wedge-shaped geometry with the internal architecture shows onlap updip and progradation of sediment on the hangingwall dip

slope (Figure 11). The discontinuous reflectors indicate the energy of deposition. This reflector shape and architecture mark the end of tilting of rift.

Late post-rift (S5)

The late stage of synrift megasequence can be recognized by the continuation of reflectors to onlap the hangingwall dip slope (Figure 11).

Postrift megasequence

Post-rift in the study area shows the parallel continuous reflector (Figure 6). These thick parallel reflectors (for about 1150 ms thick) lie above the synrift sequence and have sheet external form with almost equal thickness. The parallel pattern suggests uniform rates of deposition. The amplitude for this sequence shows the medium to high that interpreted to indicate interbedding of shales.

Syninversion megasequence

The syninversion sequence in the study area was recognized by the onlap of the reflector to the post-rift sequence and also by toplap of the reflector to the unconformity (Base Muda Unconformity) above it (Figure 6). The onlap reflection termination indicates that it was deposited during the inversion. The inversion had uplift of the synrift and postrift sequences along the fault that form the fault-propagation folds. The syninversion sequence deposited during the form of fault-propagation fold that made its reflection onlap to the previous sequence. The onlap was created on both the back-limbs and front-limbs of the fold.

Postinversion megasequence

In the study area, the start of deposition of postrift megasequence was marked by the unconformity (Base Muda Unconformity) shown in Figure 6. This sequence overlies the crest of the fold. The sequence was deposited during a period of quiescence and is the final sequence in the depositional evolution in the study area.

Isochron maps

Four isochron maps drawn for the Basement through Base Muda Unconformity horizons show that the strike of the depocenter is in a west-northwest direction and the thickest sediment for each horizon interval is placed along side of fault with north-northeast direction.

Basement – Lower Gabus interval

This interval ranges in thickness from 379 ms to 1342 ms in the depocenter basinward (Figure 12). The depocenter shows in blue area. The depocenter lies parallel to the major fault with direction west-norhtwest. The thickest sediment placed at the western part of the depocenter. The thickness increases gradually from east to the depocenter and increases slightly rapid from west to the depocenter.

Lower Gabus – Upper Gabus interval

Isochron map shows that the thickest sediment in this interval is 295 ms (Figure 13). The map shows almost equal thickness through all the area. The blue area which reveals the thickest sediment was deposited at the western part parallel to the north-south fault.

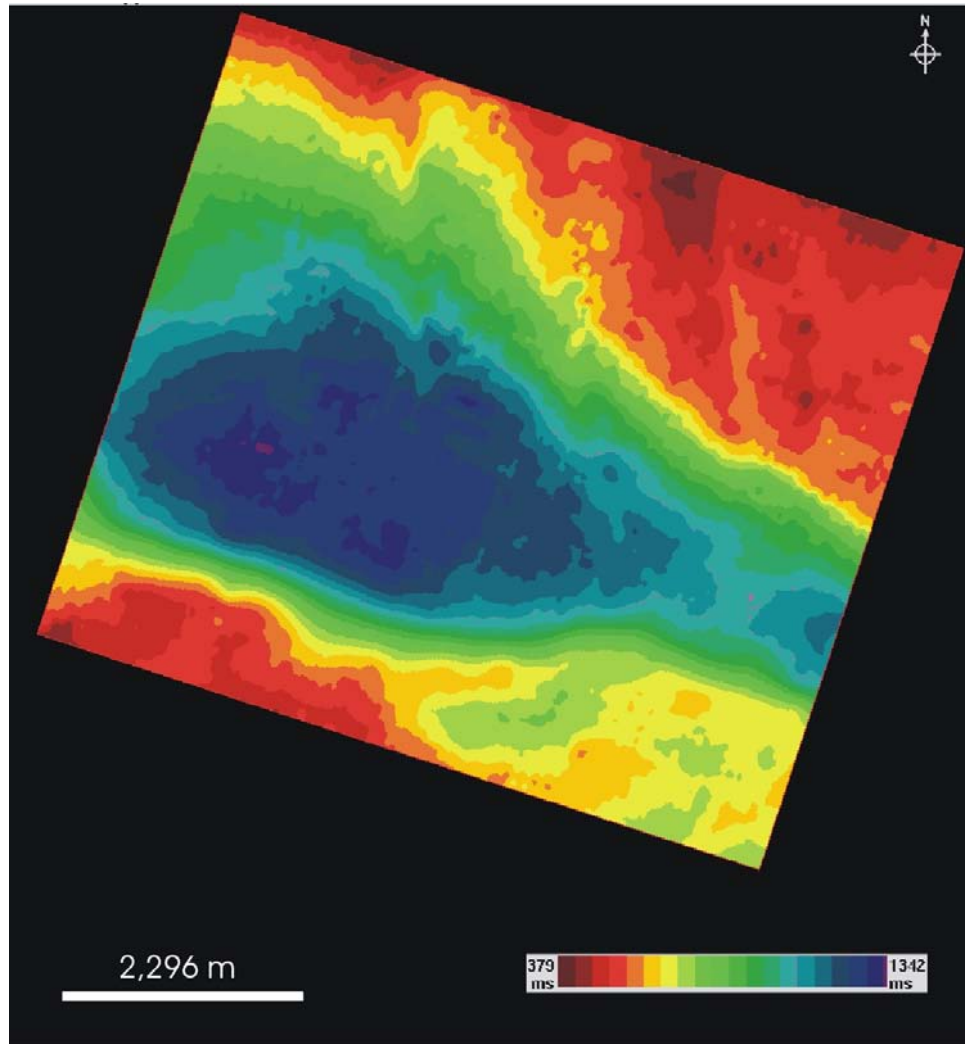


Figure 12. Isochron map of Basement – Lower Gabus interval.

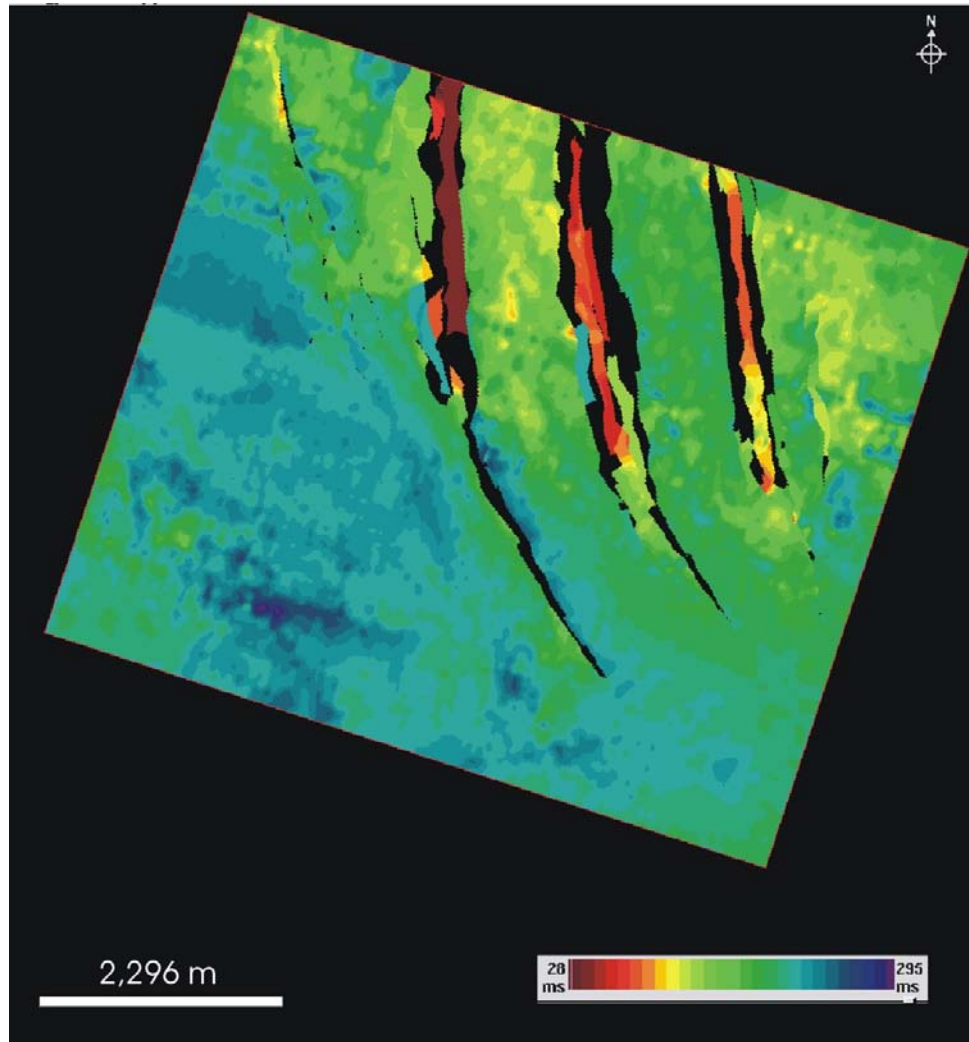


Figure 13. Isochron map of Lower Gabus – Upper Gabus interval.

Upper Gabus – Barat interval

The isochron map in this interval shows that the thickness range in all area almost the same which is it has equal thickness like what shows in the Lower Gabus – Upper Gabus interval (Figure 14). The interval has 249 ms for the thickest sediment.

Barat – Base Muda interval

The map shows the west-northwest closure that parallel to the major fault (Figure 15). The closure area shows in orange to red area has the same form with the depocenter in basement – lower gabus interval. The thickness range from 849 ms through 1213 ms. The thinnest area is in the center of closure area represent by red color that parallel to the north-south fault. It placed at both side of the fault. The thickest area shows in blue color are placed on the flank of the closure. These thickness patterns were affected by the closure form from Barat horizon against the Base Muda Unconformity at the top.

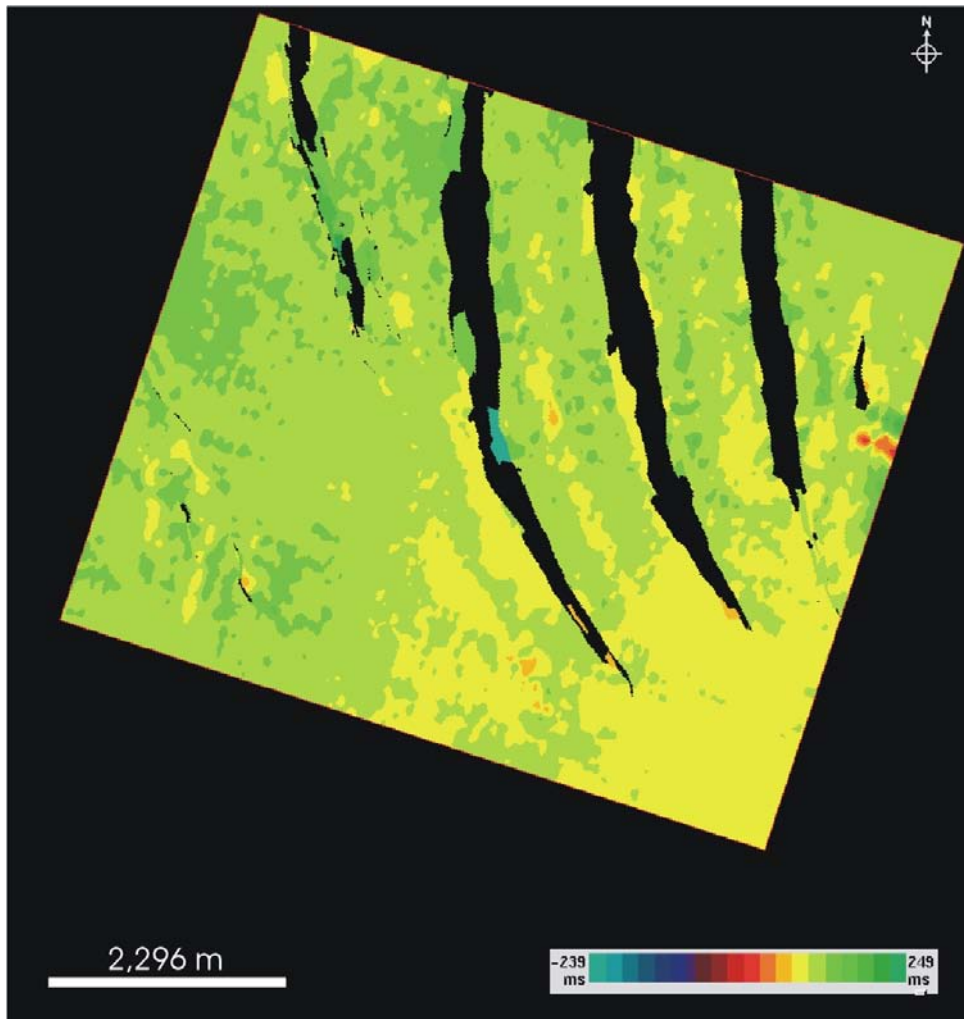


Figure 14. Isochron map Upper Gabus – Barat interval.

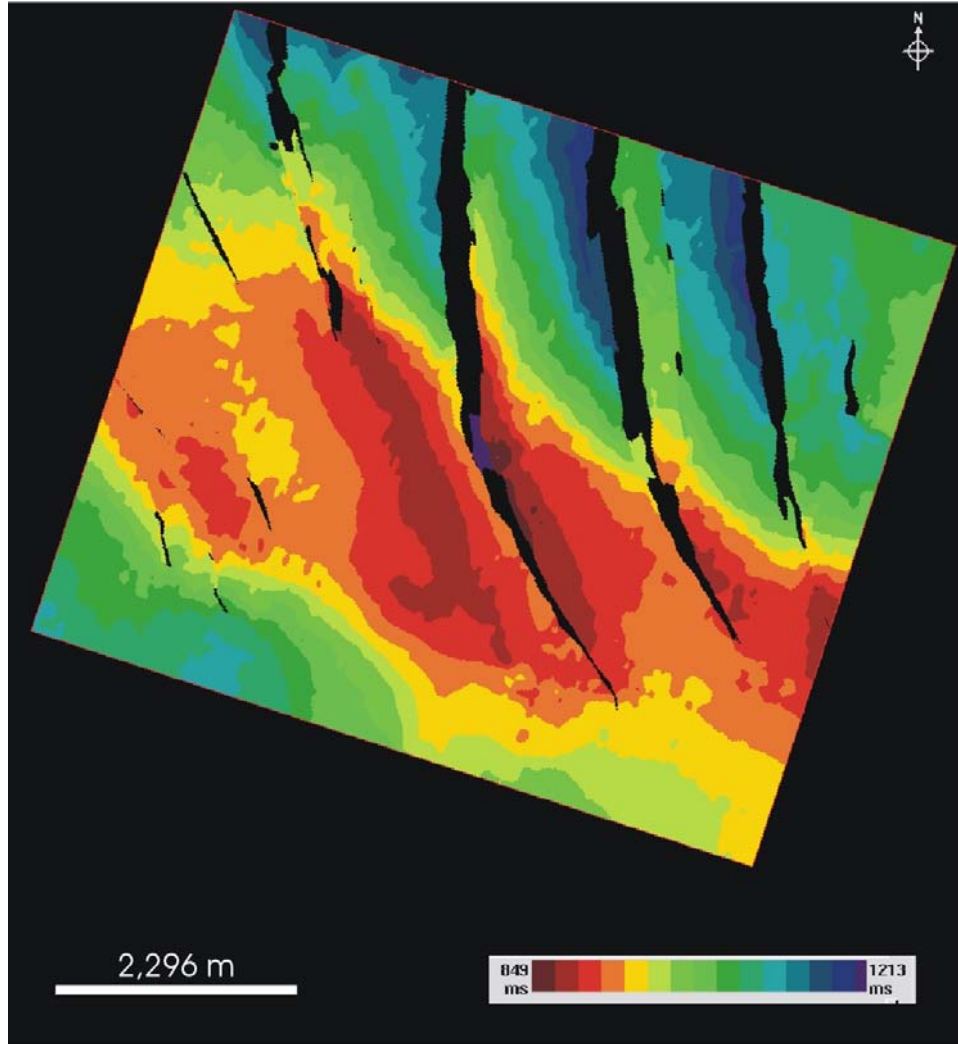


Figure 15. Isochron map Lower Gabus – Base Muda Unconformity interval.

CHAPTER V

STRUCTURAL EVOLUTION

I interpreted a series of seismic profiles and time-structure maps to establish the nature and distribution of the faults, the nature of the basement and the tectonic style that influenced the study area.

A short glance through the data revealed a half graben structure bounded by major basement fault with west-northwest-trend and dipping to the north, a series of normal fault with strike trend north-south, mostly dipping to the west and few dipping to the east and an east-west asymmetrical anticline.

Fault-propagation fold formed at the tips of a reactivated extensional fault creating an east-west asymmetrical anticline. A series of normal faults intersect this asymmetrical anticline.

Time-structure maps

I mapped the relationships among faults on all five horizons.

Basement horizon

The basement time structure map shows the synclinal-closure geometry (Figure 16). The deepest area is at 3379 ms, ranging to the shallower area, which is 2640 ms in depth. This map shows the geometry of the half graben in the area bounded by the almost east – west normal fault. This fault is dipping to the north.

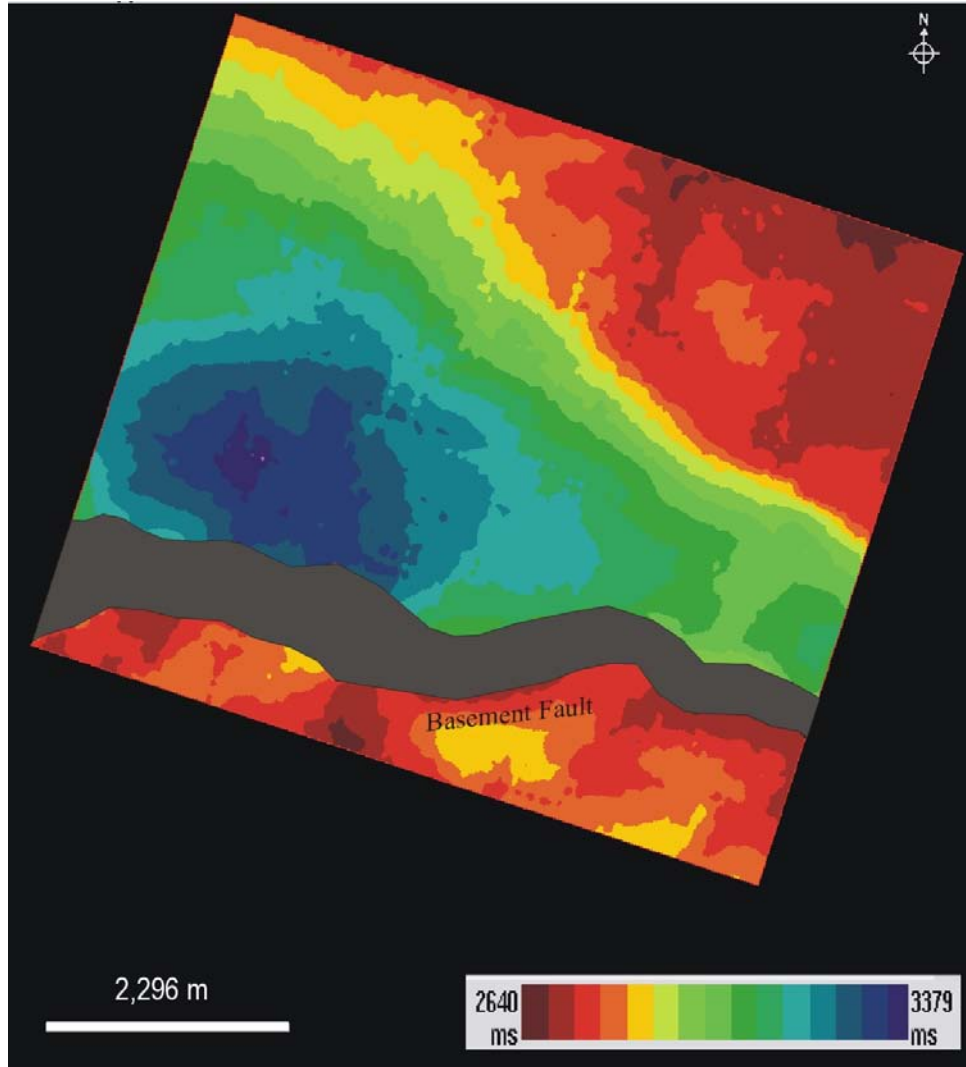


Figure 16. Time-structure map of Basement.

Lower Gabus horizon

The prominent structural features seen on this horizon include the north – south striking normal faults (Figure 17). This horizon is cut by four major normal faults which dip to the west. The normal faults shifted a little to the west compared to the Upper Gabus horizon. Horizon depth range is between 1879 ms to 2375 ms. Closure geometry in this map trends northwest – southeast.

Upper Gabus horizon

I correlated the Upper Gabus horizon in the study area. The structure follows a north – south trend. All four major normal faults in the study area cut through this horizon (Figure 18). Horizon depth ranges between 1720 ms and 2178 ms. This horizon also shows a closure that has a trend northwest – southeast. The highest part of this horizon took place in the central area and was cut through by a normal fault. The closure dips steeply to the west and gently to the east.

Barat horizon

I made a grid map of Barat horizon. The time structure map shows north-south normal faults that cut through this horizon (Figure 19). Major normal faults at the northern part of the area dip to the west while those at the southwest part dip toward the east. Two closures can be found at the side of the F3 fault.

The maximum depth of this horizon is 2078 ms while the lowest depth at this horizon is 1628 ms. The highest part of this horizon at almost the centre was cut through by a series of north – south normal faults.

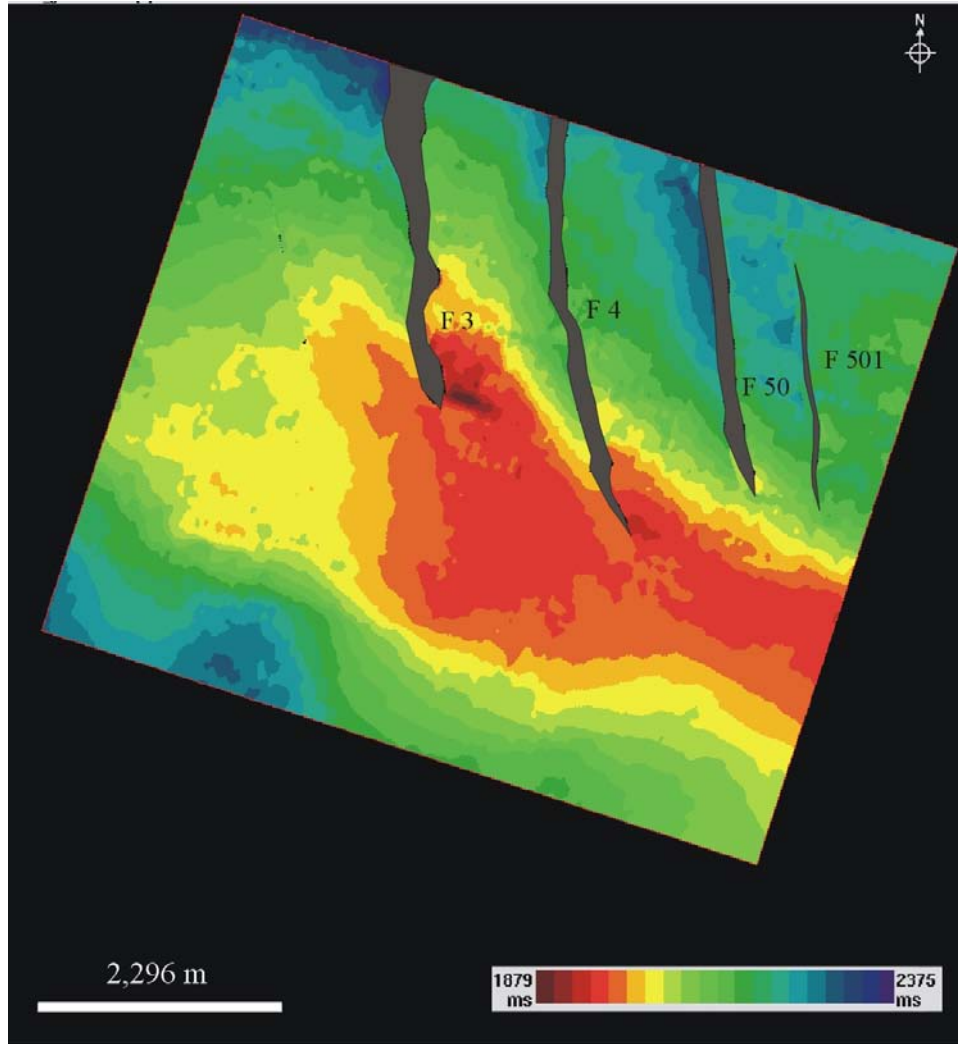


Figure 17. Time-structure map of Lower Gabus.

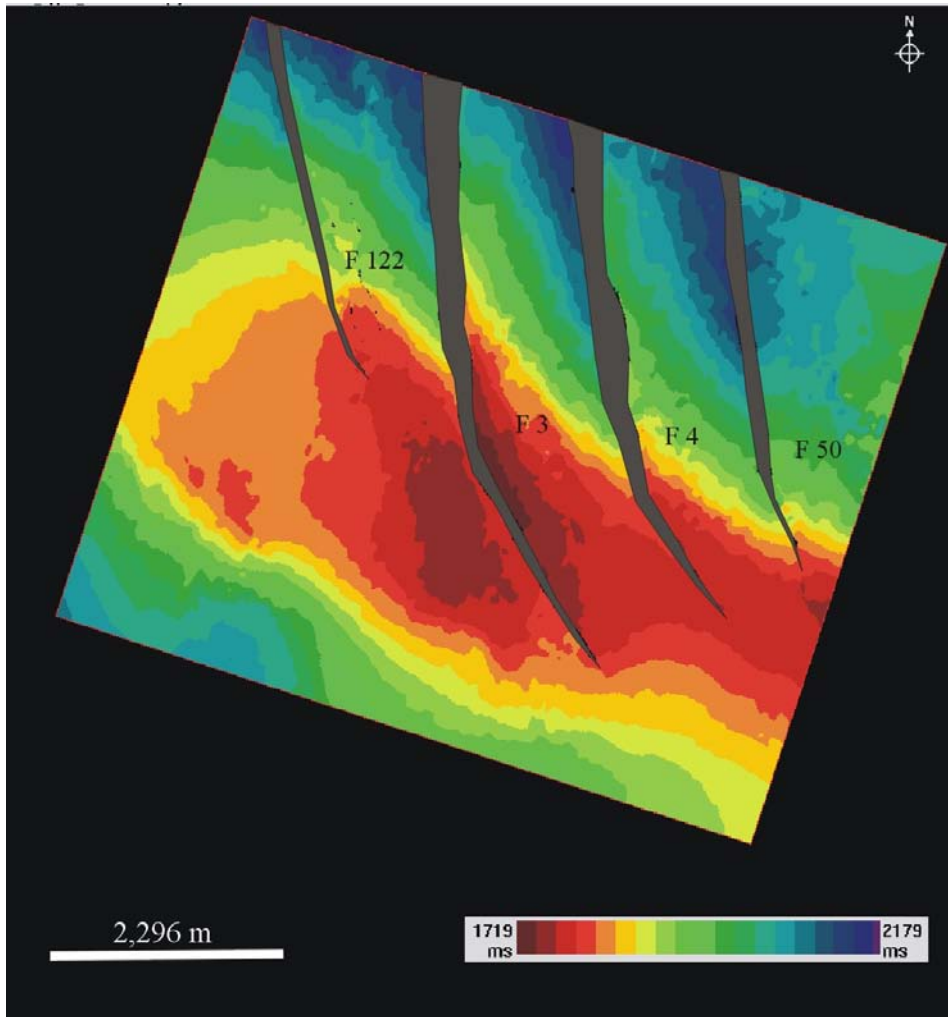


Figure 18. Time-structure map of Upper Gabus.

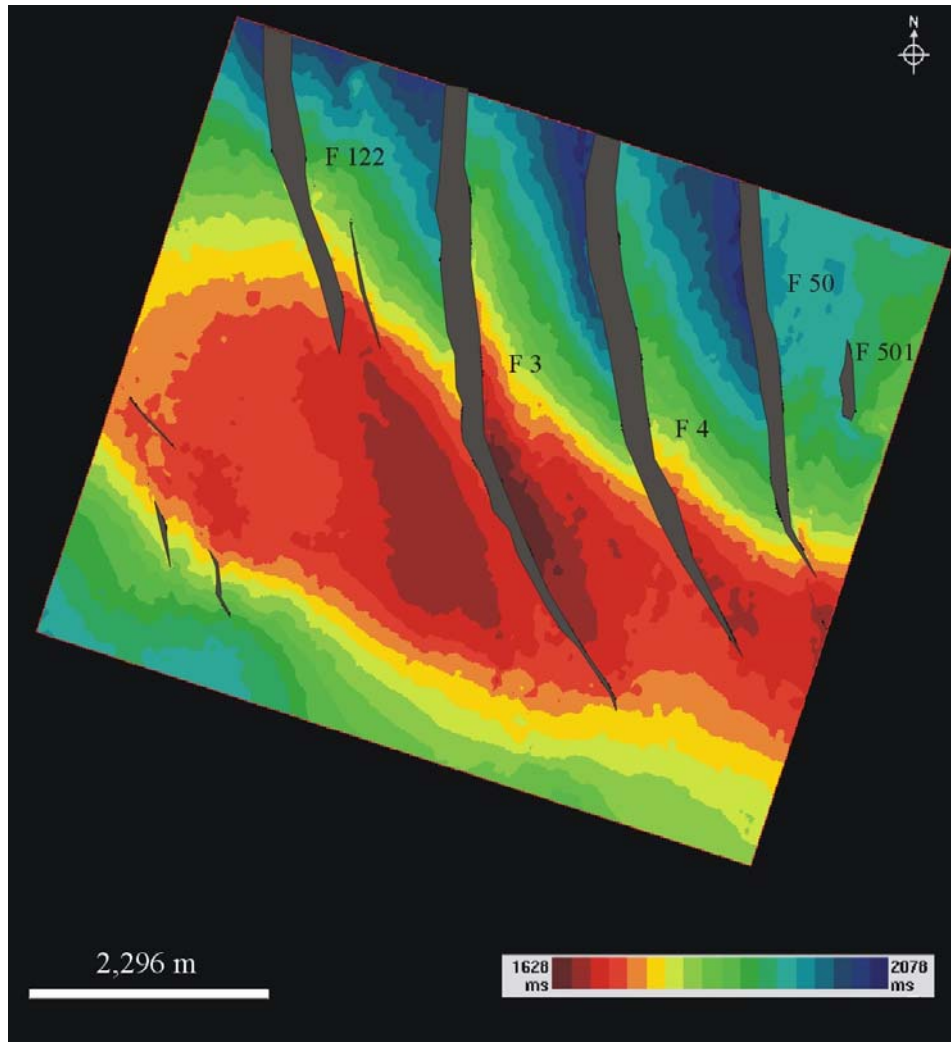


Figure 19. Time-structure map of Barat.

Base Muda Unconformity horizon

The Base Muda Unconformity horizon shows the closure with a northwest – southeast trend. Only few faults cut through this horizon (Figure 20). The normal faults are oriented in the north – south direction, dipping to the west. The horizon has a time-depth range from 756 ms to 907 ms.

Basement fault

Basement fault has a strong influence on the formation of the basin in the study area. Major west-northwest-trending basement fault have been identified from seismic data in the study area (Figure 16). The fault has planar form that dipping 60 ° to the south. This fault may have originated by transtensional stress between regional sinistral shear that accommodated extrusion of the Indochina Block (Tjia and Liew, 1996). All the sediment fills in the area lies above the hanging wall of this planar fault. The wedging shape of depositional fill shows that the depositional in this area was influencing by the movement of the fault.

Extension and inversion

Madon (1997) proposed a possible mechanism for the development of the basin in the Malay basin that I suggest can be applied also in the study area. The Malay basin has the east-trending basement faults that are oblique to the overall basin with northwest-trend. In the study area the major basement fault has also east-west trending identified from seismic data (Figure 16), rather than southwest-oriented that occurs in other

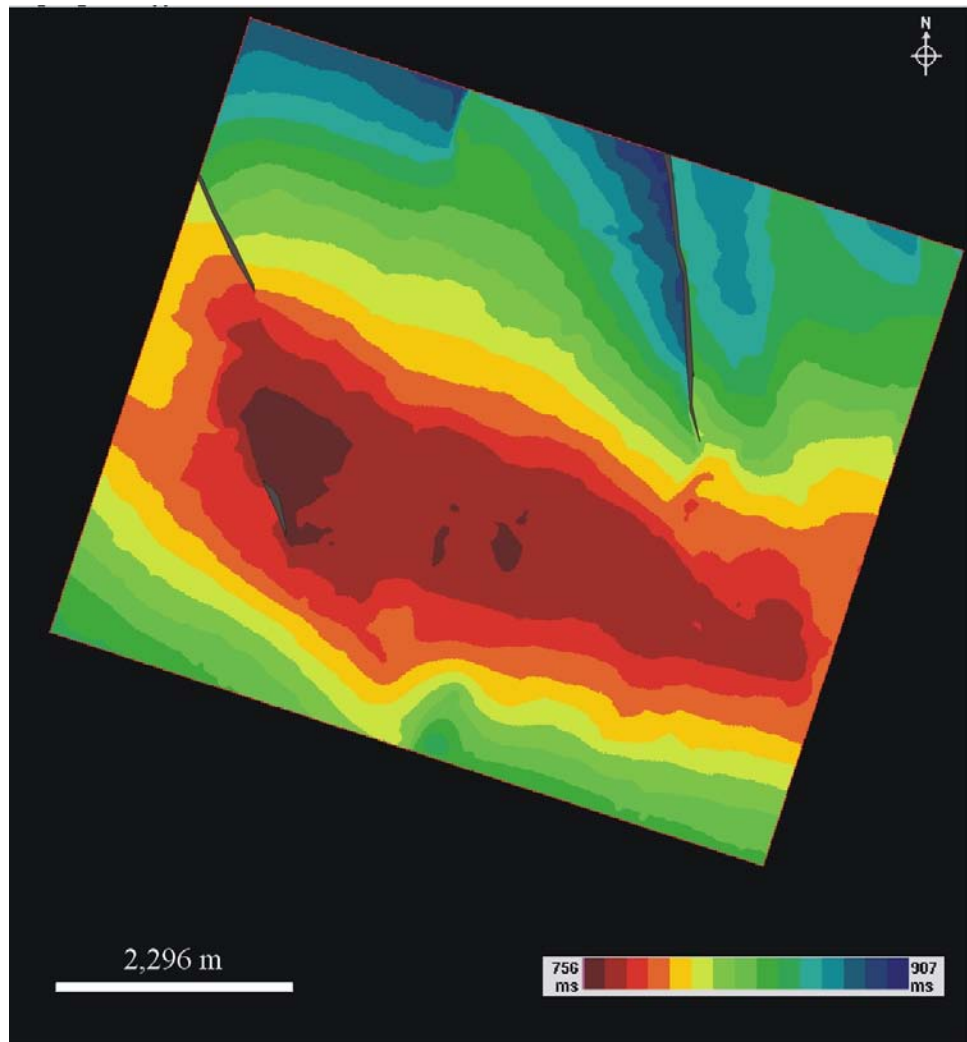


Figure 20. Time-structure map of Base Muda Unconformity.

sub-basin of the West Natuna Basin (Ginger et al., 1993). The mechanism here, that the basin was formed by distributed shear deformation of the axial shear zone (Figure 21). Madon (1997) used the block model of McKenzie and Jackson (1986) to illustrate the role of distributed continental deformation in the formation of extensional basins (Figure 22). The model suggests that the half grabens were formed by dextral oblique motion between the fault-bounded blocks, as a result of sinistral transtension of the whole zone. This extensional commenced during Eocene time (Ginger et al., 1993).

Tjia (1996) explained that the inversion in the area is caused by a reversal of the original sinistral shear. The inversion of half graben in the study area can be explained also by McKenzie and Jackson block model (Figure 22). As the original sinistral shear reversed, then the crustal blocks would rotate clockwise. This rotation will generate the north-south shortening in the graben. Fault-propagation fold was created during this process or common (ie., Sunda folds) in Sunda shelf area (Figure 23). This fold overlies an extensional half-graben that is bounded by the east-trending basement fault. The structural development of the Sunda fold in study area is illustrated in Figure 24. Other structure that suggested as inversion structure that shows in the study area was series of normal faults (Figures 25-28). These normal faults developed as secondary faults that develop during inversion.

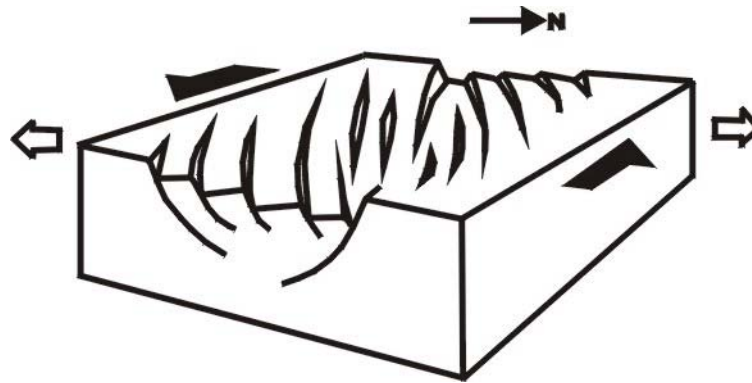
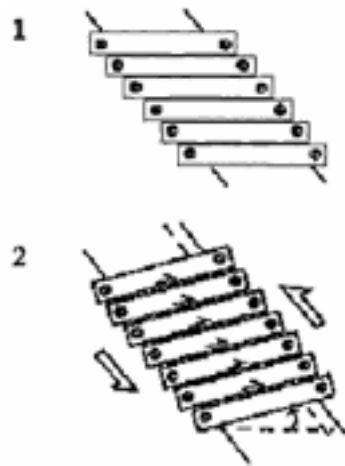


Figure 21. The schematic illustration of distributed continental deformation in the formation of extensional basins in the study area.

A. Transtension



B. Transpension

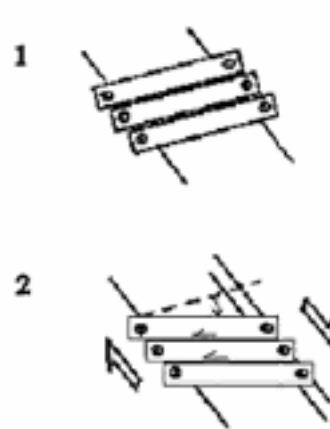


Figure 22. Block model for extension and inversion in the study area based on original concept of McKenzie and Jackson (1986).

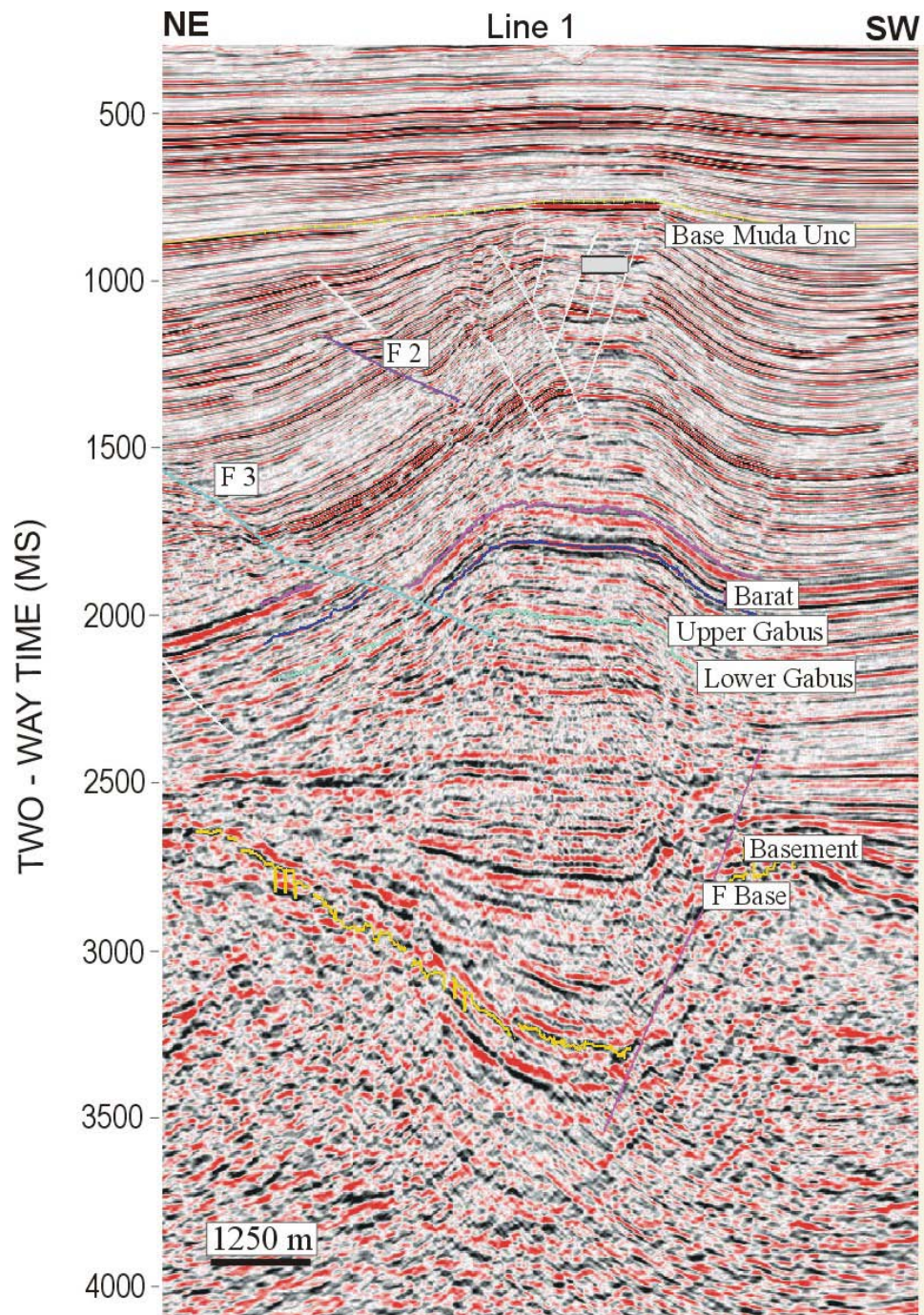


Figure 23. Line 1 showing fault-propagation fold or sunda fold. See Figure 2 for location.

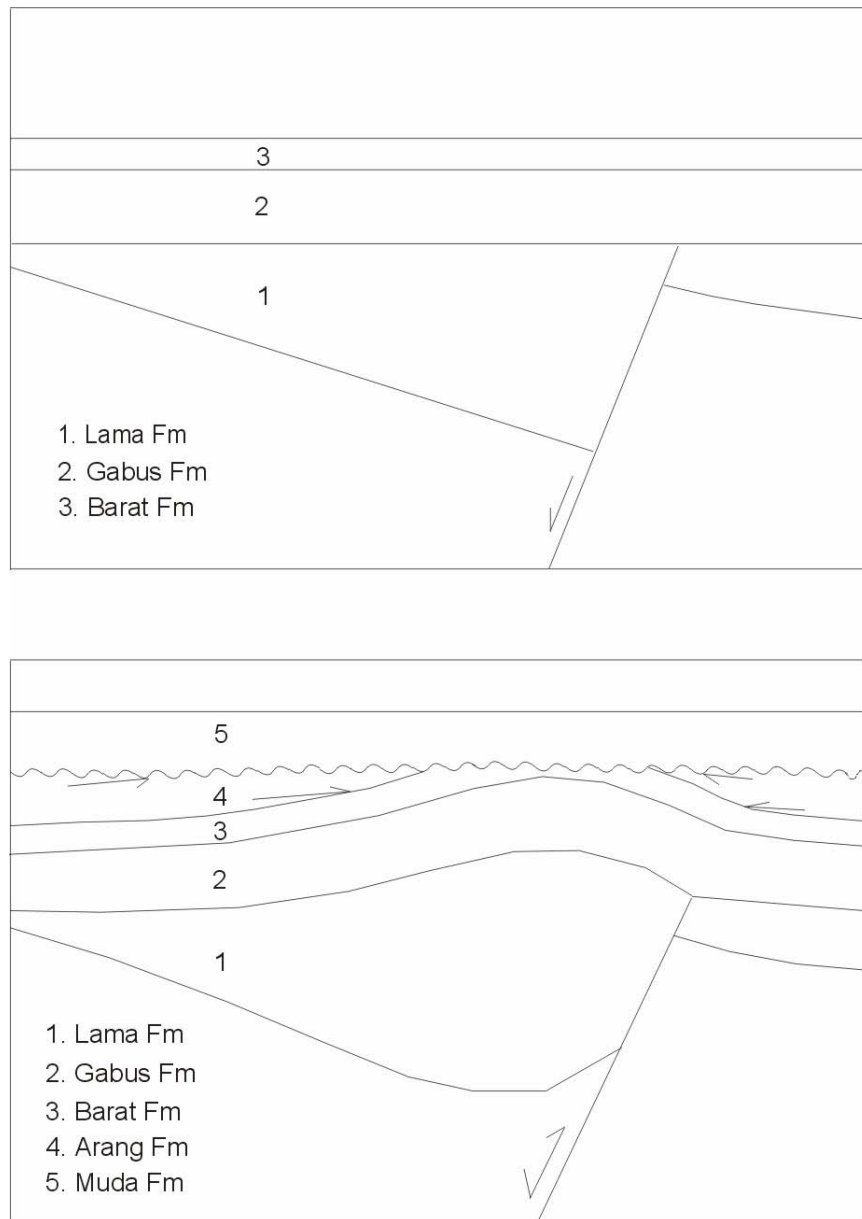


Figure 24. Structural development of Sunda fold features in study area.

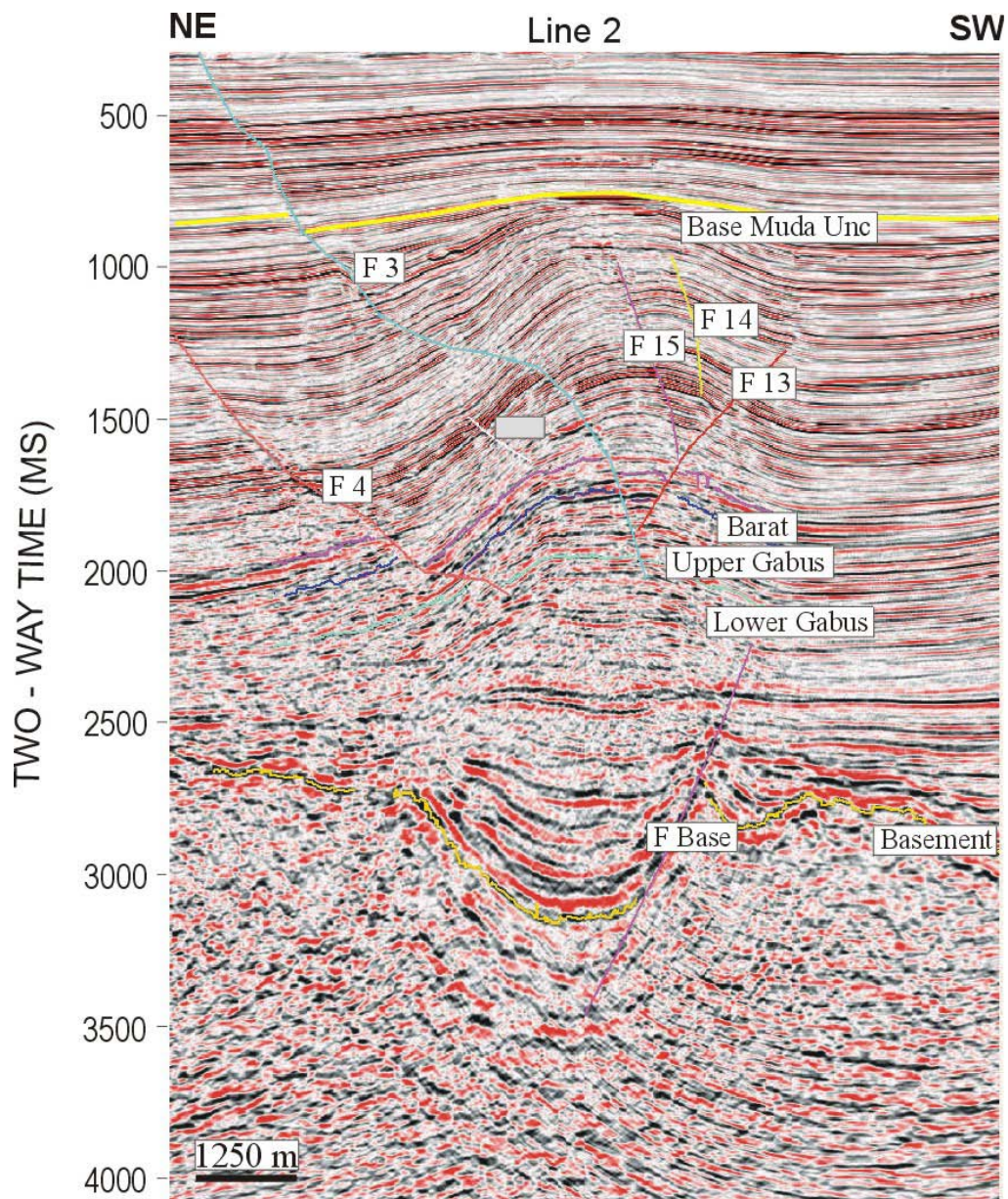


Figure 25. Line 2 showing series of normal fault that develop during inversion and basement fault. See Figure 2 for location.

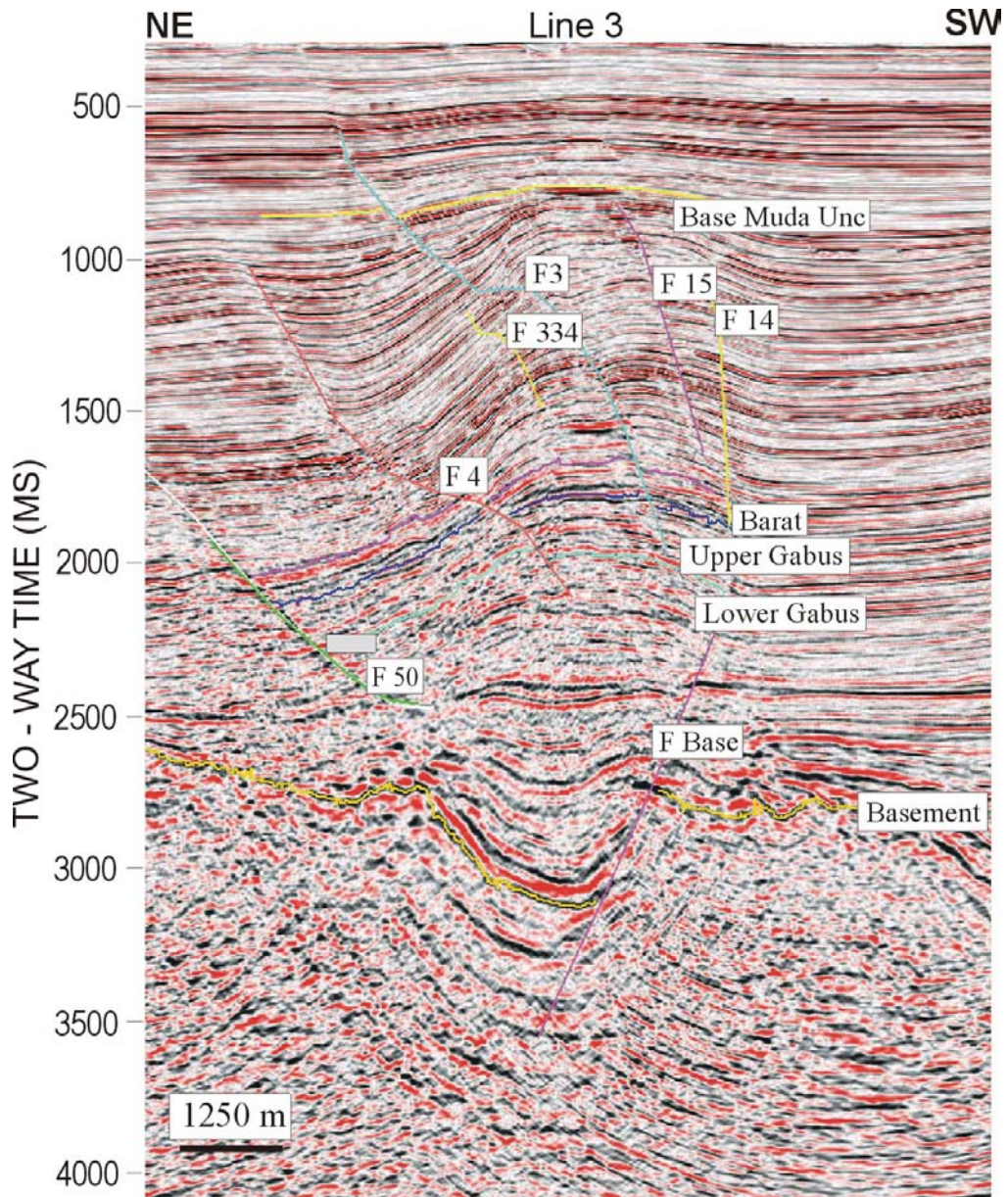


Figure 26. Line 3 showing series of normal fault and basement fault. See Figure 2 for location.

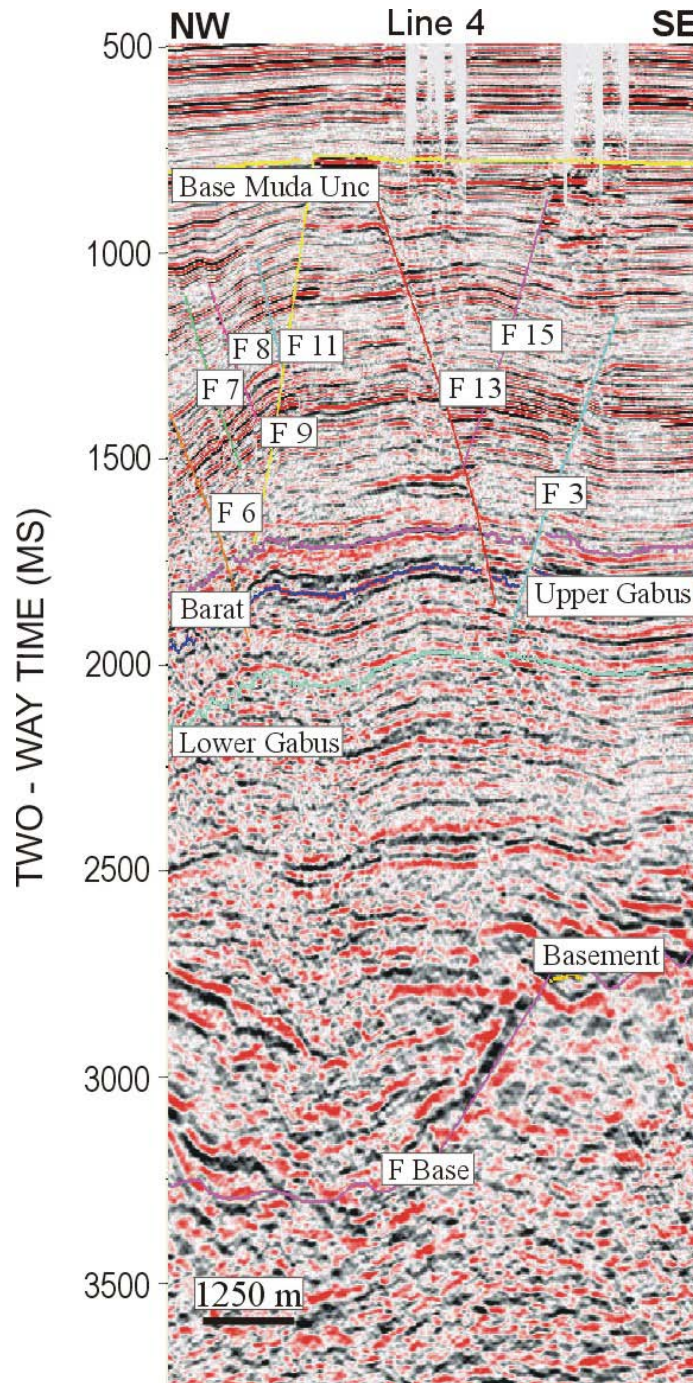


Figure 27. Line 4 showing synthetic and antithetic faults and basement fault. See Figure 2 for location.

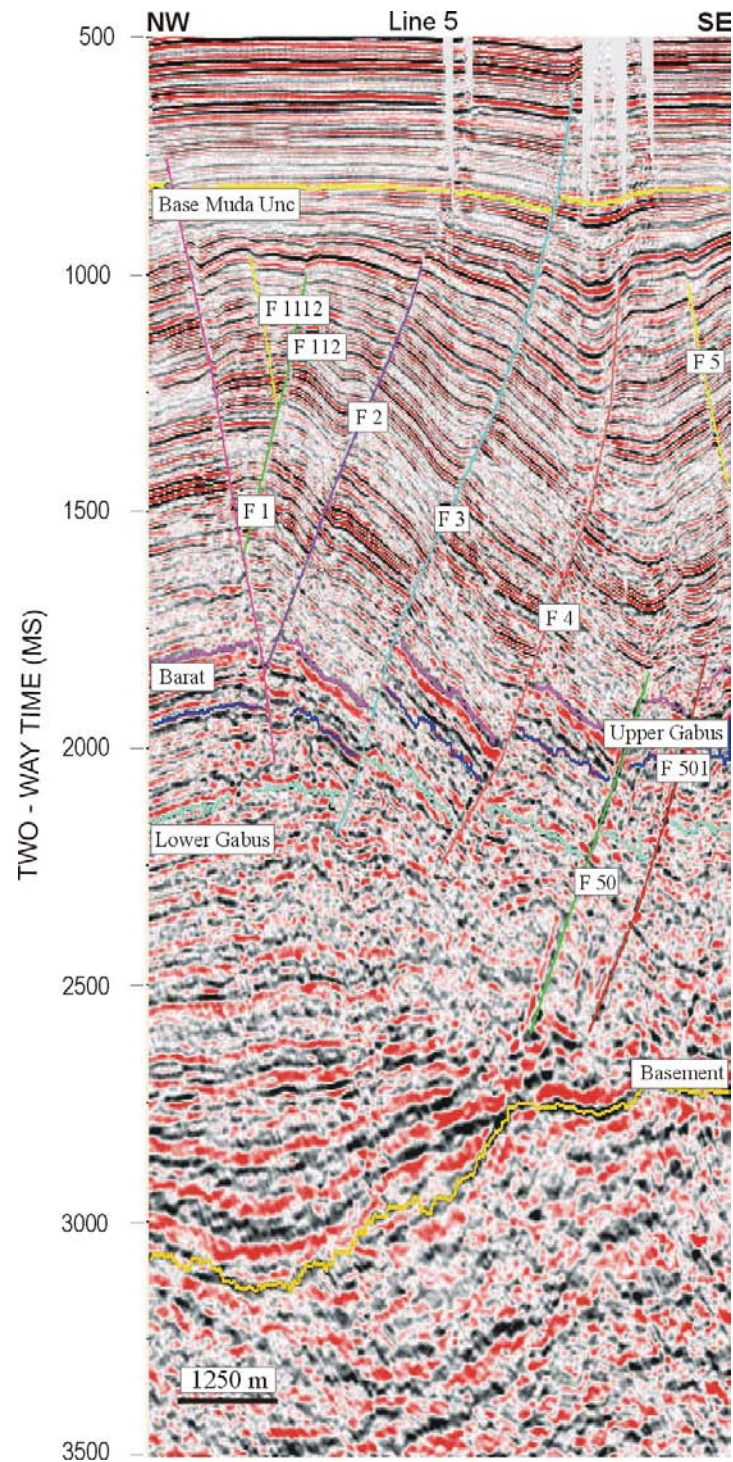


Figure 28. Line 5 showing series of normal faults. See Figure 2 for location.

CHAPTER VI

DISCUSSION

Tectonics had a great control in the expansion of the structural features and the sedimentary column in the study area. The major features involve a half graben bounded by a planar-normal fault with main orientation west-east. This planar-normal fault influenced the formation of the fault-propagation fold that post-dates the graben fill.

Model of basin development placed in regional context

Extrusion of the Indochina microplate by the Indian-Asian collision caused large blocks of continental crust to be rifted and form half grabens and grabens in West Natuna Basin by the sinistral transtensional stress. In the study area, this extrusion formed a half graben bounded by a west-east planar-normal fault (Figure 16). This agrees with the Tapponnier et al. (1982) collision-extrusion model that inferred left-lateral movement on the strike-slip faults which bounded the microplates and whose motion formed extensional basins at their ends. Later, in the early to middle Miocene, propagation of the South China Sea enabled the westward convergence of the Pacific plate. The convergence of the Indian-Australian plate from the south changed as the stress became a dextral transpressional stress that further extended the West Natuna Basin (Tjia and Liew, 1996). Compressional and transpressional stress-inverted major bounding faults created an asymmetric fault-propagation fold and a splay of normal

faults in the study area (Figure 17 - 19). These inversion structures overlie extensional half grabens that are bounded by the west-east-trending basement faults. In the study area, inversion structures also resemble series of north-south trending normal faults (Figure 25 - 28), which suggests that shortening across the half-grabens create the releasing area. A change from sinistral to dextral motion may have caused the basin to be inverted. The development of fault-propagation folds could have formed by deformation, occupying pre-existing west-northwest-east-southeast-trending en echelon half-grabens in response north-south shortening associated with the dextral shear.

Prospective traps

Prospective traps in the study area placed a series of north-south trending normal splay faults that developed by dextral transpression movement. These normal faults bound the fold that creates a closure, making them 3-way dip traps. These kinds of traps depend on reservoir juxtaposition on the upthrown block against the downthrown block in a normal fault relationship. In the study area, the Gabus and Barat reservoir formations show the development of this trap (Figure 17-19).

CHAPTER VII

CONCLUSIONS

The structure and sediment development in the study area are strongly influenced by tectonic deformation in the area. In a regional context, the basin development has undergone the transtensional sinistral shear during the rift phase, which was reactivated during the early-mid Miocene inversion as a transpressional, dextral shear.

Four periods of tectonic activity were identified in the study area by their sediment and structural architecture derived from the interpreted seismic section and the resulting maps as can be described as follows:

1. A rifting process caused the formation of half grabens. The extension stage occurred during the Eocene as indicated by Eocene sediments filling the deep grabens that were created. The rifting is bounded by normal faults that dip steeply to the north. Synrift deposition occurred as indicated by the wedging sediments. Four stages of basin evolution (rift initiation, rift climax, immediate postrift and late postrift) are characterized by this synrift deposition. Each stages shows sedimentation relation with the subsidence cause by the displacement of fault. That relationship reveals by the reflector configuration.
2. During a period of quiescence, early to late Oligocene sediments were deposited horizontally with no tectonic activity. These Postrift

sediments have a parallel, continuous reflection pattern and strong amplitude.

3. A period of compression caused the inversion of sediment in structural lows in early to middle Miocene time. This is illustrated in the inversion structure by development of the Sunda fold shown in Figure 24. Syninversion deposition occurred, as indicated by onlap and toplap.
4. A major erosion (Base Muda Unconformity) was followed by a period of quiescence and deposition of postinversion sediment.

The trap play is related to the tectonic deformation across the area. A structural closure developed along a series of north-south-trending, normal splay faults that formed as a result of dextral transpression in mid to late Miocene time.

REFERENCES CITED

- Daly, M. C., M. A. Cooper, I. Wilson, D. G. Smith, and B. G. D. Hooper, 1991, Cenozoic plate tectonics and basin evolution in Indonesia: Marine and Petroleum Geology, v. 8, p. 2-21.
- Eubank, R. T., and A. C. Makki, 1981, Structural geology of the central Sumatra back-arc basin: Indonesian Petroleum Association, 10th Ann Conv, p. 153-196.
- Ginger, D. C., W. O. Ardjakusumah, R.J. Hedley, and J. Potheary, 1993, Inversion history of the West Natuna Basin: examples from the Cumi-Cumi PSC: Proceedings of the 17th Annual Convention of the Indonesian Petroleum Association, v. I, p. 635-658.
- Gulf Resources (Kakap) Ltd., 2000, PSC summary and prospect and lead inventory, Kakap PSC Offshore West Natuna, Unpublished Report.
- Harding, T. P., 1990, Identification of wrench faults using subsurface structural data: criteria and pitfalls: The American Association of Petroleum Geologists Bulletin, v. 74, p. 1590-1609.
- Longley, I. M., 1997, The tectonostratigraphy evolution of SE Asia, *in* Fraser, A.J., Matthews, S.J. and Murphy, R.W. (eds), Petroleum Geology of Southeast Asia: Geological Society Special Publication, v. 126, p. 311-339.

- Madon, M. B. H., 1997, The kinematics of extension and inversion in the Malay Basin, Offshore Peninsular Malaysia: Bulletin Geological Society of Malaysia, v. 41, p. 127-138.
- Pollock, R. E., J. P. Hayes, K. P. Williams, and R. A. Young, 1984, The petroleum geology of the KH Field, Kakap, Indonesia: Proceedings of Indonesian Petroleum Association, v. 13, p. 407-423.
- Prosser, S., 1993, Rift-related linked depositional systems and their seismic expression, *in* Williams, G.D. and Dobb, A. eds., Tectonics and seismic sequence stratigraphy: Geological Society Special Publication, no. 71, p. 35-66.
- Pupilli, M., 1973, Geological evolution of South China Sea Area – tentative reconstruction from Borderland Geology and well data: Proceedings of Indonesian Petroleum Association, v. 2, p. 223-241.
- Roberts D. G., 1988, Basin evolution and hydrocarbon exploration in the South China Sea, *in* Wagner, H. C., Wagner, L. C., Wang, F. F. H., and Wong, F. L., editors, Petroleum Resources of China and Related Subjects: Houston, Texas, Circum-Pacific Council for Energy and Mineral Resources Earth Science Series, v. 10, p. 157-177.
- Tapponier, P., G. Peltzer, A.Y. Le dain, R. Armijo, and P. Cobbold, 1982, Propagating extrusion tectonics in Asia: new insight from simple experiments with plasticine: Geology, v. 10, p. 611-616.

- Tjia H. D., and K. K. Liew, 1996, Changes in tectonic stress field in northern Sunda Shelf basins, *in* R. Hall, and D. J. Blundell, eds., Tectonic evolution of Southeast Asia: Geological Society Special Publications, London, Geological Society of London, p. 291-306.
- Wirojudo, G. K., and A. Wangsosantiko, 1985, Tertiary tectonic evolution and related hydrocarbon potential in the Natuna Area: *Energy*, v. 10 (3/4), p. 433-455.
- White Jr., J. M., Wing and R.S. Wing, 1978, Structural development of the South China Sea with particular reference to Indonesia: *Proceedings of Indonesian Petroleum Association*, v. 7, p. 159-174.

VITA

Name	Maria Fransisca Meirita
Mailing Address	Perum Pemda Jatiasih Bekasi Blok A8 No.6 Jatiasih, Bekasi, Indonesia 17423
Working Address	Exploration Department Gulf Indonesia Resources Ltd. – CONOCOPHILLIPS Indonesia Inc. Mulia Tower 4-5 th floor, Jalan Gatot Subroto, Jakarta, Indonesia
Educational Background	B.S. in geology, Trisakti University, April 1998. M.S. in geophysics, Texas A&M University, August 2003.
Professional Organization	American Association of Petroleum Geologist (AAPG), Society of Exploration Geophysicist (SEG).
Experience	Junior Geologist Gulf Indonesia Resources Ltd. December 1999 – July 2000